北海道南西部における島弧地殻の地震波速度構造と深部低周波地震
Seismic velocity structure beneath southern Hokkaido and its relation to crustal deep low-frequency earthquakes

*椎名 高裕[1]、高橋 浩晃[1]、岡田 知己[2]、松澤 暢[2]
*Takahiro Shiina[1], Hiroaki Takahashi[1], Tomomi Okada[2], Toru Matsuzawa[2]

1. 北海道大学大学院理学研究院附属地震・火山研究観測センター、2. 東北大学大学院理学研究科附属地震・噴火予知研究観測センター
1. Institute of Seismology and Volcanology, Graduate School of Science, Hokkaido University, 2. Research Center for Prediction of Earthquakes and Volcanic Eruptions, Graduate School of Science, Tohoku University

The crustal deep low-frequency earthquakes (CDLFE) are often occurred beneath active volcanoes in Japan (e.g., Takahashi and Miyamura, 2008). Additionally, some CDLFEs showing the similar characteristics for those observed beneath volcanoes are also detected in non-active volcanic areas, such as a fault zone (e.g., Ohmi and Obara, 2002). However, relations between the CDLFEs and volcanoes and regular earthquakes occurred in the arc crust have not been revealed in clearly.
In southern Hokkaido, the CDLFEs are observed beneath both of active volcanoes and non-active volcanic areas, which corresponds to shallow swarm-like activity of the regular crustal earthquakes. This indicates southern Hokkaido is an interesting region for understanding the relations between the CDLFE and near surface phenomena, including volcanoes and crustal earthquakes. In this study, therefore, we investigate seismic velocity structure beneath southern Hokkaido in detailed and then discuss the relations of them based on the obtained heterogeneous structure.
In order to estimate the seismic velocity, we applied the double-difference tomography technique (Zhang and Thurber, 2003; 2006). From the earthquake catalogue by Japan Meteorological Agency, we collected 15,645 earthquakes which occurred in the period from March 1st, 2003 to June 15th, 2016. A magnitude range of the earthquakes was 1.5-6.5. The number of travel time data is 306,335 for P wave and 242,093 for S wave.
In addition to characteristic structures as imaged in previous studies (e.g., Kita et al., 2010; Niu et al., 2016), the obtained results clearly show the low-velocity zones are distributed at depths of about 20-40 km beneath around the active volcanoes and generating regions of the CDLFEs. Correspondingly, high-Vp/Vs ratio is calculated at the depths. In contrast, high-velocity zones are widely determined at a depth of 10 km, while reductions of seismic velocity from surroundings are obtained near the active volcanoes. The crustal earthquakes which involves shallow seismic swarms occurred above the DLFEs seems to be located within the high-velocity zones. The obtained spatial variations of the seismic velocity demonstrate that the CDLFEs are posited at transition zones of velocity and Vp/Vs ratio, proposing that presence and migration of fluids or melts would attribute for their triggering (e.g., Ukawa and Ohtake, 1987). Additionally, heterogeneity that associate with the upper crust and correspond to the CDLFEs seem to closely link to the subsurface phenomena at above the CDLFEs: crustal earthquakes occurred in the upper crust are facilitated in the high-velocity zones and active volcanoes are located within the low-velocity area those compared from surroundings.

キーワード：地震波速度、深部低周波地震、群発地震、北海道
Keywords: seismic velocity, deep low-frequency earthquakes, seismic swarm, Hokkaido

The 2016 Northern Ibaraki Prefecture Earthquake (M_j 6.3) Rupturing the Fault of the Large Earthquakes in 2011 Again

*内出 崇彦[1]、大谷 真紀子[1]、高橋 美紀[1]、今西 和俊[1]
*Takahiko Uchide[1], Makiko Ohtani[1], Miki Takahashi[1], Kazutoshi Imanishi[1]

1. 産業技術総合研究所 地質調査総合センター 活断層・火山研究部門
1. Geological Survey of Japan, National Institute of Advanced Industrial Science and Technology (AIST)

The 2011 Tohoku-oki earthquake (M_w 9.0; hereafter referred to as "mainshock") activated the seismicity in many areas not only in Japan but also all over the world. In particular, in the Fukushima Hamadori and the northern Ibaraki prefecture (hereafter, "N. Ibaraki") areas, northeast Japan, the rate of the seismicity with normal faulting mechanisms jumped to high, although the seismicity had been inactive before the mainshock. This is because the preexisting east-west extensional stress regime was significantly strengthened by the mainshock [*Imanishi et al.*, 2012]. In the N. Ibaraki area, a large earthquake with Japan Meteorological Agency magnitude (M_j) of 5.7 ("Event 2011a") occurred just 8 minutes after the onset of the mainshock. Another large earthquake (M_j 6.1; "Event 2011b") struck on March 19, 2011, 8 days after the mainshock. On April 11, 2011, an M_j 7.0 earthquake struck the Fukushima Hamadori area, on the north of the N. Ibaraki area. Afterward the seismicity has been attenuating with time.

On December 28, 2016, a large earthquake (M_j 6.3, "Event 2016") occurred in the N. Ibaraki area. The interferograms of the SAR data for Events 2011a and 2011b [*Kobayashi et al.*, 2011] and Event 2016 [*Geospatial Information Authority of Japan (GSI)*, 2017] are very similar to each other, implying the similarity in earthquake rupture processes.

We analyzed rupture processes of the Events 2011a, 2011b, and 2016 by finite-fault slip inversion analyses using strong-motion data from KiK-net, K-NET, and F-net. Our fault models indicate that the Events 2011a and 2016 ruptured the ground surface as reported by field observations [*Aoyagi et al.*, 2015; *Geological Survey of Japan*, 2017], whereas Event 2011b did not. Note that this does not contradict the SAR analysis [*Kobayashi et al.*, 2011] and the field observation [*Aoyagi et al.*, 2015], because they have no temporal resolution to distinguish the deformation occurred on March 11 (Event 2011a) and 19 (Event 2011b). Overall the rupture areas of two events in 2011 and the Event 2016 are overlapping and similar to each other.

Why could the large earthquakes occur on the same fault twice in such a short time, almost 6 years? Since the fault strength recovers quickly [e.g., *Dieterich*, 1972], a stress loading and/or a fault weakening are required. According to the strain change inferred from the GNSS data by GEONET of GSI, the east-west extensional plain strain on the ground surface was rapidly increased after the mainshock, however afterward the east-west compressional strain rate has been observed, which seems to contradict the occurrence of the normal faulting large earthquake. Detail will be studied by a seismicity analysis based on the ETAS model [*Uchide*, this meeting].

It is probable that the large earthquakes in the N. Ibaraki area occurred due to the coseismic and postseismic deformation of the Tohoku-oki mainshock. Since the postseismic deformation generally attenuate with time, the seismic activity will also be decay. A quantitative assessment will require numerical simulations with a precise rheology model as well as seismic and geodetic observation to monitor the seismicity and crustal deformation.

キーワード：茨城県北部地域、内陸地震
Keywords: Northern Ibaraki Prefecture Area, Inland Earthquake

Very short recurrence interval of M~6 earthquakes within the common fault zone

*加藤 愛太郎[1]、酒井 慎一[1]、飯高 隆[1]、小原 一成[1]
*Aitaro Kato[1], Shin'ichi Sakai[1], Takashi Iidaka[1], Kazushige Obara[1]

1. 東京大学地震研究所
1. Earthquake Research Institute, the University of Tokyo

Immediately after the 2011 M9.0 Tohoku-Oki, an intensive seismicity characterized as normal faulting was induced near the pacific coast in the southern part of Tohoku region [Kato et al., 2011, 2013]. From the end of March in 2011 to the present, we have continued to precisely monitor the seismicity deploying a dense seismic network consisting of around 60 portable stations equipped with short-period sensors (the station interval is around 4 km). The seismicity has continued after the Tohoku-Oki earthquake, while the seismicity rate has gradually decreased. On 28 December, 2016, a magnitude of 6.3 earthquake took place in this region, and boosted up an intensive seismicity. We relocated aftershocks following this event, using seismic waveforms retrieved from the dense seismic network. The relocated earthquakes almost overlapped with those triggered after M6.1 earthquake on 19 March, 2011. A sharp alignments of earthquakes dipping toward SW was clearly imaged. This indicates that two magnitude 6 earthquakes occurred on the common fault zone. This idea is supported by spatial p pattern of surface displacements revealed by InSAR technique (GSI, 2017). It is very surprising that M6 earthquakes took place with very short recurrence interval along the common fault zone.

Estimation of spatiotemporal distribution of interplate slip after the 2003 Tokachi-oki earthquake incorporating viscoelastic relaxation

*伊東 優治[1]、西村 卓也[2]
*Yuji ITOH[1], Takuya NISHIMURA[2]

1. 京都大学大学院理学研究科、2. 京都大学防災研究所
1. Graduate School of Science, Kyoto University, 2. Disaster Prevention Research Institute, Kyoto University

The 2003 M_w 8.0 Tokachi-oki earthquake is an interplate earthquake along the Kurile trench. Its postseismic deformation has been observed by GNSS [e.g., Miyazaki et al. 2004]. Estimation of spatiotemporal afterslip is a key to clarify the healing process after large earthquake. Because the postseismic deformation should be caused by both viscoelastic relaxation and afterslip, it is important to incorporate both effects for the modeling. In this study, we estimated a spatiotemporal interplate slip for about 7.5 years following the 2003 event as well as the coseismic slip of the 2003 and M 6-7 class earthquakes simultaneously. We included a viscoelastic response of interplate slip in the estimation of the slip.
For the data analysis, we corrected the effect of the 1993 Hokkaido-Nansei-oki earthquake for the observed GNSS data in Hokkaido by using the model of Ueda et al. [2003]. The secular velocity before the 2003 event was estimated from the corrected data and removed from the postseismic data. And then, we removed a seasonal variation and displacements of the M6-7 events in the postseismic period. Finally, we down-sampled the residual time series with an interval of 1-6 months. We used about 7.5 years long GNSS data until the 2011 Tohoku-oki earthquake.
For the modeling of postseismic deformation, we constructed a model consisting of the coseismic slip of the 2003 and the following M6-7 class events, interplate slip including afterslip following these events and viscoelastic relaxation. We assumed the two-layers viscoelastic structure estimated by Itoh and Nishimura [2016] to estimate interplate slip distribution.
A preliminary result shows large postseismic slip occurred in the up-dip and down-dip extensions of the coseismic slip region and implies an interplate coupling had not been recovered to that before the 2003 event at the time of the 2011 event.

キーワード：2003年十勝沖地震、GNSS、余効変動、余効すべり、粘弾性緩和
Keywords: The 2003 Tokachi-oki earthquake, GNSS, Postseimsic deformation, Afterslip, Viscoelastic relaxation

日本海富山トラフ剪断帯とアムールプレート東縁の現生テクトニクス
Toyama Trough Shear Zone of Japan Sea and active tectonics along Japan margin of Amur Plate

*竹内 章[1]
*Akira Takeuchi[1]

1. 富山大学理学部
1. Faculty of Science, University of Toyama

わが国では，1995年兵庫県南部地震以降，日本海側と内陸のひずみ集中帯において地殻地震が発生する状況が続いており，加えて2011年東北地方太平洋沖地震の発生を受け，海溝型巨大地震と島弧内帯の活断層型地震との密接な関連性が議論されている。また，国の海洋基本計画に基づく海洋資源開発や海陸両域を統合した地殻構造探査，地震・測地観測などが稠密に実施され，データが集積されてきた。

こうした背景を踏まえて，日本海盆南東部・大和海盆東部・富山トラフを含む日本海東縁海域における資源探査ならびに地震津波調査の資料をコンパイルし，主として鮮新世以降の中央日本北部のネオテクトニクス，とくに富山トラフから北部フォッサマグナ地域にかけての東西日本島弧系の境界域および日本海東縁変動帯の挙動を断層活動史解読の観点から総括した。その結果，当該海域の断層ブロック構造が明らかになり，日本海盆および大和海盆の東縁部に南北方向の大規模な剪断帯をもつ２段階の背弧拡大過程を裏付ける知見が得られた。それにもとづき断層活動史を編み，日本海東縁変動帯の仮説を検証する作業により，つぎの２点が解明された。

a）活断層および現在は活動を停止している断層を含む地体構造が明らかになった。とくに，富山トラフを構成する断層群のうち，南北走向の断層群（右ずれ剪断帯）が大和海盆東縁まで追跡された。
b）大和海盆拡大の第２時階末葉（17 Ma頃）とされる西南日本の時計回転の際には，富山トラフの南北剪断帯で左ずれをともなう開口変位があった。

本州弧の構造発達史を踏まえた地殻変動帯の形成過程については，日本海拡大のメカニズムおよび現在のプレート境界の位置との関連において，つぎのように結論される。

1）日本海での拡大から短縮への地殻変動モードの移行は，中部日本のネオテクトニクスにおいても画期的転換であった。この転換は本州の東西で発生時期に差異がみられ，フィリピン海プレートの沈み込みの影響下で起きた西南日本弧側の東西系褶曲は、能登半島では後期中新世に生じた。 東北日本弧側では，富山トラフ南部と信越堆積盆を特徴付けるNE-SW系断層褶曲構造が顕著になったのは、かなり遅れて４Ma以降であった。これはアムールプレートの東進開始が契機とみられる。

2) 対象地域の断層分布については，富山トラフ剪断帯を境にアムール・オホーツク間のプレート境界に沿った相対運動の様相，すなわち本州中部での島弧ー島弧衝突を「する側」と「される側」の変動として解釈できる。衝突される側の日本海盆の東縁を含む東北日本弧内帯は全域で「正反転」が卓越する。衝突する側では、後期白亜紀に活動した断層をもつ西南日本弧の内陸で「転換」が、また背弧堆積盆で「反反転」がみられる。なお、大和トラフでは拡大に関与した断層の再活動が認められない。

3）現在の本州では，新潟ー神戸ひずみ集中帯が西南日本弧の内陸部から東北日本弧日本海側にわたって観測され，糸魚川ー静岡構造線と交差する。これを定常的に沈み込む太平洋プレートの上盤で生じた東北日本弧と西南日本弧の衝突・合体（あるいはDiffuse zoneの拡大，本州弧の復活）を象徴する現象とみれば，この構

造帯の発現は第四紀中期にさかのぼる。

キーワード：日本海、ネオテクトニクス、富山トラフ、反転テクトニクス、アムールプレート
Keywords: Japan Sea, neotectonics, Toyama Trough, tectonic inversion, Amur Plate

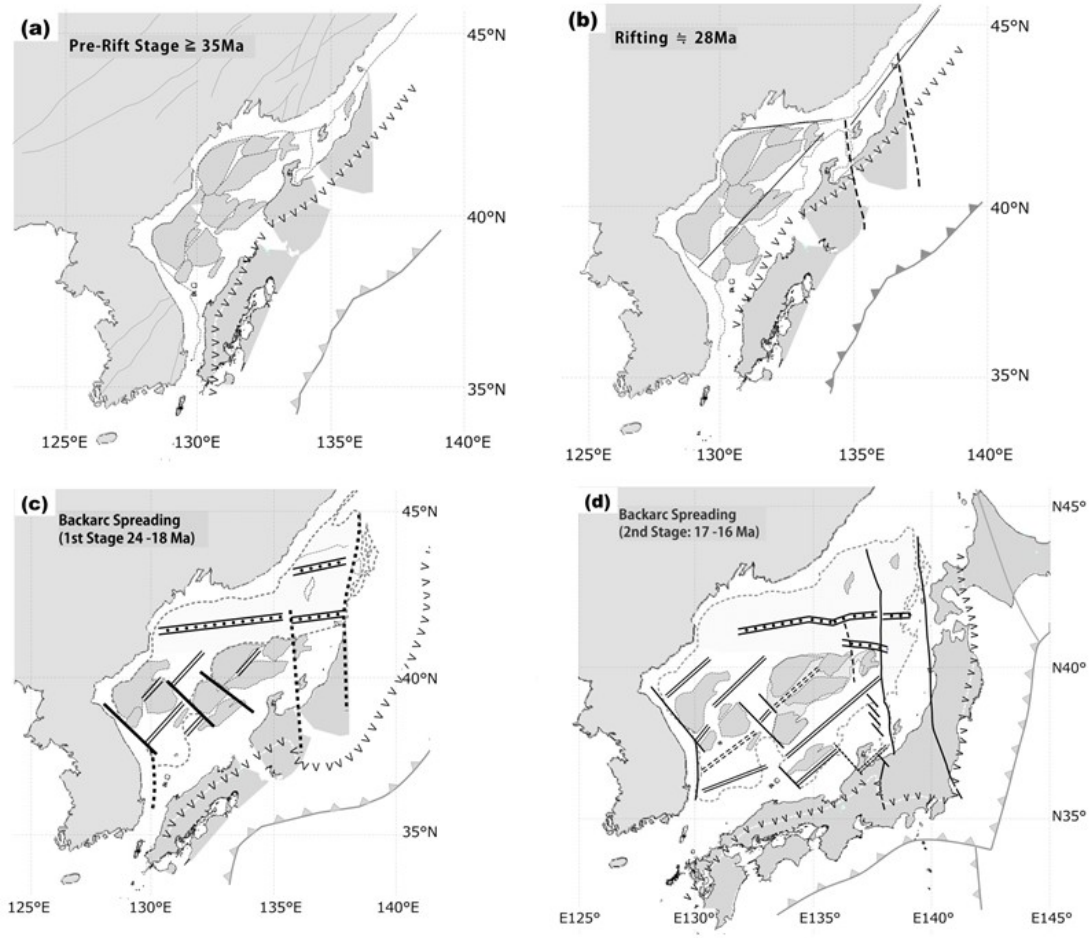

A tectonic scenario explaining a progressive opening of Japan Sea and rotation of Southwest Japan

Deformation of the Philippine Sea Slab and its Implication for the Tectonics of Central and Western Japan

*深畑 幸俊[1]
*Yukitoshi Fukahata[1]

1. 京都大学防災研究所
1. Disaster Prevention Research Institute, Kyoto University

In this study, I estimate the contraction rate in central and western Japan from deformation of the Philippine Sea slab. Usually a slab subducts with little deformation as indicated by the slab contour lines that are nearly parallel to the trench in most subduction zones. Little deformation of slabs is reasonable from the view point of elastic energy.
However, the Philippine Sea slab is an exception; large deformation of it beneath central Japan has been estimated from hypocenter distributions, receiver function analyses, and seismic waveform tomography. It is considered that such large deformation is caused by east-west contraction, which prevails in the most area of Japanese islands.
Observed characteristics of the deformation of the Philippine Sea slab are as follows: (1) little deformation in the west of the Kii strait; in the east of the Kii strait, (2) little deformation in the region between the Nankai trough and the coast line, (3) progressively accumulated deformation to the north of the coast line. Little deformation in the west of the Kii strait is consistent with less number of active faults and their commonly slow displacement rates.
The deformation rate of the Philippine Sea slab related to the characteristic (3) is estimated to be about 5 - 10 km/Ma. This estimate would give the minimum contraction rate in the crust of the Chubu and Kinki district, Japan.

キーワード：フィリピン海スラブ、地殻変動、中部日本
Keywords: Philippine Sea slab, crustal deformation, central Japan

The characteristics of the brittle deformation structure causing “Crustal strain-rate paradox” in the Niigata-Kobe Tectonic Zone

*田村 友識[1]、大橋 聖和[1]
*Tomonori Tamura[1], Kiyokazu Oohashi[1]

1. 山口大学創成科学研究科
1. Yamaguchi University Graduate School of Sciences and Technology for Innovation

Introduction

NKTZ has been known as the high strain rate zone causing right lateral movement and the slip rate of the zone is estimated to 12mm/y by GNSS observation (Ohzono et al., 2011). On the other hand, the total slip rate based on geological survey of the active faults in the NKTZ (the Atostugawa fault, Ushikubi fault and Takayama-Oppara fault) is only 6mm/y. This result is not equal to the result of the GNSS observation. This is called “Crustal strain-rate paradox”. However, the rate of the Kokufu fault zone which is distributed in the southward area of the Atostugawa fault system is not considered when discussing this paradox. The Kokufu fault zone has not yet been investigated by the topographic or geological survey in detail and clarified the brittle deformation structure. The aim of this study is to clarify the brittle deformation structure in and around the Kokufu fault zone by using topographic and geological approaches and discuss what causes the paradox in the NKTZ.

Topographic and Geological Overview

In the study area, active faults such as Unehata fault and Toichigawa fault which is belonging to the Kokufu fault zone are distributed. There are also fault taraces indicating active faults in the Inagoe area. The Hida metamorphic rocks, Tedori formation, Nohi rhyolite, Funatsu granite are distributed in the study area. According to geological map (Geological Survey in Japan, 1975) in the study area, there are many geological faults or geological boundary faults.

Results

In the Miborotani outcrop (Loc.1), the fault is composed of 10 cm yellow-orange fault gouge and fault breccia. Strike and dip of the fault gouge is N65E85S and the plunge of the slicknline on the fault surface plunges 10 to the south. This fault outcrop is composed of Unehata fault.
In the Kurigatani outcrop (Loc.2), the fault is composed of 20 cm blue gray fault gouge and fault breccia. Strike and dip of the fault gouge is N25E60S and of the slicknline on the fault surface plunges 18 to the south. This fault outcrop is in the area located about 200 meters far away from the active faults.
In the Soutsuitani outcrop (Loc.3), the fault is composed of the fracture zone including fault gouge and fault breccia. Strike and dip of the fracture zone is N89W75N.

Discussion

By the topographic and geological surveys, we found many faults in the off-fault area which is the area far away from the active faults. These faults cause the “Crustal strain-rate paradox”. Therefore, it is important for considering “Crustal strain-rate paradox” to clarify the brittle deformation structure around the Kozkufu fault zone.

キーワード：新潟-神戸構造帯、脆性変形構造
Keywords: Niigata-Kobe Tectonic Zone, brittle deformation structure

2009年から2014年までの新潟-神戸歪集中帯北東部のcoda Qの時間変化
Temporal variation in Coda Q in the northeastern part of Niigata-Kobe Tectonic Zone in 2009-2014

*道場 正伸[1]、平松 良浩[2]
*Masanobu Dojo[1], Yoshihiro Hiramatsu[2]

1. 金沢大学大学院自然科学研究科、2. 金沢大学理工研究域自然システム学系
1. Graduate school of Natural Science and Technology, Kanazawa University, 2. Faculty of Natural System, Institute of Science and Engineering, Kanazawa University

大地震が発生すると地殻の応力状態が変化することによって地震活動度や地殻の不均質性が変化する。Hiramatsu et al. (2000) と Sugaya et al. (2009) では、1995年兵庫県南部地震による丹波地方のcoda Qの時間変化が報告されている。Padhy et al. (2013) では、2011年東北地方太平洋沖地震によって引き起こされた東北地方の太平洋沿岸でのcoda Qの時間変化が報告されている。その一方、Tsuji et al. (2014) では、2011年東北地方太平洋沖地震による濃尾断層帯周辺のcoda Qの統計的に有意な時間変化は報告されていない。そこで、本研究では2009年1月から2011年2月 (period I) と2012年1月から2014年10月 (period II) の新潟-神戸歪集中帯北東部のcoda Qの時間変化を調べることとする。

本研究ではperiod I で646個、period II で2194個の地震を解析した。これらのイベントはマグニチュードが1.8以上、震源の深さは30 km以浅である。震央から30 km以内の観測点のデータからAki and Chouet (1975)の一次後方散乱モデルを適用してcoda Qを求める。

period I と period II のcoda Qを比較したところ、log (coda Q^{-1})の変化は13%以内であった。log (coda Q^{-1})の空間分布の時間変化に注目すると、低周波数帯で log (coda Q^{-1})が増加した領域は火山領域の周辺にあり、中周波数帯や高周波数帯では目立った変化は観測されなかった。しかし、それぞれの観測点での log (coda Q^{-1})の時間変化についてt検定を実施した結果、統計的に有意な変化は認められなかった。したがって、新潟-神戸歪集中帯北東部では、2011年東北地方太平洋沖地震によるcoda Qの時間変化は統計的に有意なものではないと考えられる。

キーワード：2011年東北地方太平洋沖地震、高歪速度領域
Keywords: the 2011 Tohoku earthquake, high strain rate zone

Tectonic Loading of the Atera Fault inferred from Dense GNSS Observation

*熊谷 光起[1]、鷺谷 威[2]、松多 信尚[3]
*Koki Kumagai[1], Takeshi Sagiya[2], Nobuhisa Matsuta[3]

1. 名古屋大学環境学研究科附属地震火山研究センター、2. 名古屋大学減災連携研究センター、3. 岡山大学大学院教育学研究科
1. Earthquake and Volcano Research Center Graduate School of Environmental Studies, Nagoya University, 2. Disaster Mitigation Research Center, Nagoya University, 3. Okayama University Graduate School of Education

The Atera Fault is in the east of Gifu Prefecture is a major active fault in Japan. The fault is left-lateral strike slip in the NW-SE direction, consistent with E-W trending P-axes of earthquakes. The geological slip rate is 2~4mm/year and the seismic recurrence interval is estimated to be about 1700 years. However, a hydraulic fracturing experiment and the GEONET F3 solution suggested the Atera Fault undergoes right-lateral displacement (Yamashita et al. 2010), which is not consistent with the long-term activity of the fault. In this study, We study crustal deformation and stress filed of the Atera Fault by GNSS observation and numerical modeling. For this purpose, we install using dense GNSS network near the fault trace with an average interval of several kilometers in order to reveal detailed crustal deformation pattern. Based on GNSS daily coordinate from is January 2014 to October 2016, we calculate average horizontal velocity at each GNSS site. The velocity pattern is dominated by the postseismic deformation of the 2011 Tohoku-oki earthquake and interplate coupling at the Nankai Trough. Therefore we correct overall deformation pattern in order to extract displacements related the fault activity. After the correction, a left-lateral displacement pattern is identified. Then I conclude the Atera Fault is dislocating left-lateral. Comparison with the elastic dislocation model showed that our observation is consistent with geological estimated fault slip rate (2~4mm/year) and the seismologic layer thickness (~15km) in central Japan. We also evaluate the topographic perturbation on the crustal stress filed under a lithostatic equilibrium. The calculation suggests that the topographic effect is significant at shallow depth (~5km) and greatly affects the crustal stress pattern. The calculated maximum compressional axis at the hydraulic fracturing site depth of 350m is directed to the north-south with a differential stress of about 1.70~3.86MPa, consistent with the observation. The results demonstrate that the motion of the Atera Fault is left-lateral, consistent with the regional stress filed. It is also suggested that tectonic loading of a crustal fault does not change even under elastic perturbation due to postseismic deformation and interplate coupling. It is essential to estimate stress flied at the seismogenic depth in order to discuss fault activity.

キーワード：阿寺断層、GNSS、応力蓄積、応力、ブシネスク
Keywords: Atera Fault, GNSS, Tectonic Loading, stress, Boussinesq

Strain concentration zone in the San-in area analyzed by GNSS data

*水戸川 司[1]、小暮 哲也[1]
*Tsukasa MITOGAWA[1], Tetsuya KOGURE[1]

1. 島根大学大学院総合理工学研究科
1. Interdisciplinary Faculty of Science and Engineering, Shimane University

Micro-earthquakes are distributed along the coast of the Japan Sea in the San-in area located in the north of the Japan Median Tectonic Line. Large earthquakes such as the 2000 Tottori Western Earthquake (M7.3) and the 2016 Middle Tottori Earthquake (M6.6) occurred in this area. Both earthquakes occurred along unidentified faults. This suggests that the information about the distribution of active faults is not enough to predict the occurrence place of earthquakes.
GNSS Earth Observation Network System (GEONET) was launched by the Geospatial Information Authority of Japan (GSI) in 1994. GEONET revealed the pattern of the surface crustal movement. Sagiya et al. (2000) used the technique and found Niigata-Kobe Tectonic Zone (NKTZ) where strain rate was large. Actually, many earthquakes occur along this zone. Therefore, strain rate in San-in area is also expected to be large. The purpose of this study is to find strain concentration zones in the San-in area considering the distribution of strain rate in high resolution calculated from GNSS data.
We used the GNSS daily coordinates (so-called the GEONET F3 solution) provided by GSI (Nakagawa et al., 2009). We calculated only the trend component of displacement rate although GNSS data itself includes the effects of some parameters such as annual and semi-annual trend of deformation or step deformation due to earthquakes. The displacement rate at each observation point was aligned to lattice point with interval of 0.1 degree obtained by Nearest Neighbor method in Generic Mapping Tools (GMT). The maximum rate of shear strain was calculated by differentiating displacement rate with respect to the distance among each lattice point. Results show that the distribution pattern of the strain rate changes with time and observation period. The largest strain rate of about 200 nanostrain/yr is found in Middle Tottori and around Mt. Sambe, which is an active volcano in Middle Shimane.

キーワード：ひずみ速度、GNSS、山陰地域
Keywords: Strain rate, GNSS, San-in area

Fault distribution in the southern part of the small earthquake swerm zone along the Sanbe to Miyoshi, central Chugoku region, Japan

柳楽 武志、内田 嗣人[1]、佐野 達也[1]、*向吉 秀樹[1]
Takeshi Nagira, Hideto Uchida[1], Tatsuya Sano[1], *Hideki Mukoyoshi[1]

1. 島根大学大学院総合理工学研究科地球資源環境学領域
1. Department of Geoscience Interdisciplinary Graduate School of Science and Engineering, Shimane University

NW-SE trending small earthquakes swarm are observed along a zone of the center part of Shimane Prefecture to the northern part of Hiroshima Prefecture. Direction of the small earthquakes swarm is almost parallel to the aftershock distribution of the 2000 Western Tottori Earthquake (October 2000, M 7.3). The aftershock area of the 2000 Western Tottori Earthquake has experienced the M5 earthquake 8 times from 1950 until the main shock. In a similar fashion, small earthquakes swarm zone from the Sanbe-Miyoshi swarm earthquake zone has also experienced the M5 earthquake 12 times from 1950 until present day.
These similarity implies existence of concealed active faults along the Sanbe-Miyoshi swarm earthquake zone. Although previous studies in the aftershock area of the 2000 Western Tottori Earthquake revealed development of more than 1000 NW trending faults, the Sanbe-Miyoshi swarm earthquake zone has never been studied.
The purpose of this study is to understand the fault distribution and clarify their features in the southern part of the Sanbe-Miyoshi swarm earthquake zone.
The study area is a 6 km square around Kimita town in Hiroshima Prefecture. The investigation method is to record the fault by field survey and make thin section from sampled fault rock and observed the microstructure.
In the study area, Cretaceous rhyolite-dacite tuff and granite-porphyry, Paleogene biotite granite and granite-porphyry and Neogene Bihoku group (mudstone, sandstone, conglomerate) is exposed.
Total of 366 faults were observed in the study area. The orientation of these faults were concentrated in the about N56˚W trend and inclined at a high angle to the north and south direction. In addition, strike of the fault was concentrated in the Northeastern part of the study area about N60˚W, and in the Southwestern part about N20˚W. The fault rocks in the northeastern part of the study area were hardly consolidated, but most of those of southwestern part were unconsolidated. The cutting relation of the fault was confirmed in the northeastern part of the study area. The fault of the NE trend was often cut the fault of NW trend.
In the southwestern part of the study area, fresh fault gouge was observed in a NW trending fault. Cutting relationship of the faults in this area were hardly observed.
This fresh fault is specific to the NW trending fault in the southwestern part, and unidentified in the NE trending fault.
Occurrence of fault rock in this study area implies that the fault system in the northeastern part is older than the those of southwestern part because consolidated fault rocks is commonly formed at the deeper part than the fault gouge. Cutting relationship of the faults in the northeastern part of the study area indicates NE trending fault is developed later than the NW trending fault. In the southwestern part of the study area, fresh fault gouge was observed only in the NW trending fault implies the NW trending fault is formed later than the NE trending faults.
Orientation of faults in this study area was concentrated at about N 56˚W. But the distribution direction of small earthquake swarm in this study area is concentrated on about N40˚W. Deviation of orientation of faults and distribution aftershock is reported at the aftershock area of the Western Tottori Earthquake and

the deviated faults is thought to be Riedel shear planes of Early stages of fault development. However, the trend of faults and fault rocks in this study area is slightly different from the aftershock area of the Western Tottori Earthquake. For example, most fault rocks in the northeastern part of the study area were consolidated (Most of the fault rocks in aftershock area of the Western Tottori Earthquake were unconsolidated), and the faults in the southwestern part are concentrated in N20˚W. From this fact, this study is thought to be faults related to aftershock distribution different from the study of previous research.

キーワード：群発微小地震帯、山陰歪集中帯
Keywords: microearthquake swarm, Sanin shear zone

鳥取県西伯郡 南部町東部から伯耆町における断層分布と断層岩の特徴
Distribution and characters of faults in the eastern Nanbu town and Houki town, Tottori Prefecture, western Japan

*佐野 達也[1]、内田 嗣人[1]、大久 雅貴[1]、柳楽 武志、向吉 秀樹[1]
*Tatsuya Sano[1], Hideto Uchida[1], Masaki Oku[1], Takeshi Nagira, Hideki Mukoyoshi[1]

1. 島根大学大学院総合理工学研究科地球資源環境学領域
1. Department of Geoscience Interdisciplinary Graduate School of Science and Engineering, Shimane University

2000年鳥取県西部地震は明瞭な活断層が検出されていない地域で発生した地震であり、この地域では他の活断層に比べ未成熟な断層系が発達している可能性がある。先行研究では余震域で1000条以上の断層が確認され、WNW－ESE走向とNE－SW走向に卓越することが明らかとなった。しかしながら、余震域とその外側の断層の相違点・特徴は理解されていない。

よって、本研究の目的は鳥取県西伯郡南部町東部から伯耆町において地表地質踏査を行い、余震域と余震域外の断層系の分布および断層岩の特徴の類似点および相違点について明らかにすることとした。

調査地域は鳥取県西伯郡南部町東部から伯耆町までの範囲とした。この地域には根雨花崗岩帯と呼ばれる白亜紀後期の花崗岩が分布している。花崗岩は主に粗粒黒雲母花崗岩であり、アプライト質～ペグマタイト質花崗岩、西部には斑状黒雲母花崗岩、北東部には鮮新世のかんらん石玄武岩と洪積世の河岸段丘堆積層も分布する。また、玄武岩質～安山岩質岩脈、流紋岩質岩脈、アプライト質岩脈が花崗岩中に貫入している。

本研究の調査地域西部ではN84°E82°NとN45°W77°N、中央部ではN66°E78°N、N88°E90°、N70°W88°N、やや東部ではN68°W88°N、東部ではN32°W86°Nへの断層姿勢の卓越がみられた。西部と中央部では白色の断層岩が多く、やや東部と東部では、桃色を呈するものが多い。

また、西部では破砕されたような母岩が確認でき、そのような地点をダメージ帯とした。ダメージ帯には熱水変質を受けたようなカタクレーサイト質の基質が確認され、母岩の岩片が一定の方向に配列している。ダメージ帯では断層岩1cm 以下のNE走向の断層を多数形成し、時折、その多くの断層を切断するようにして幅2㎝以上あるNW走向の断層岩が確認される。また、NE走向の断層の配列は中央部でもみられた。

断層姿勢を比較すると、調査地域西部・中央部は余震域の断層と類似している。東部は小町－大谷リニアメントと走向が類似している。色相を比較すると、調査地域西部・中央部は先行研究で言われる余震域の特徴に類似しており、東部は先行研究で言われる余震域の外側の特徴に類似している。このことから、調査地域西部・中央部は余震域と同じ断層系に属すると考えられる。東部は小町－大谷リニアメントに関連する断層だと考えられる。よって、2000年鳥取県西部地震の断層系は震央から余震分布に直交する方向に7㎞の広がりがあると考えられる。しかし、これほど断層が広がることは考えにくい。調査地域西部・中央部では、ひずみ集中帯の影響を受けている可能性もある。

キーワード：2000年鳥取県西部地震
Keywords: 2000 Western Tottori earthquake

Fault zone development in the aftershock area of the 2016 Kumamo earthquake, Kyushu, Japan

*小林 健太[1]、高橋 啓太[2]、鈴木 俊[2]、大橋 健治[1]、香取 拓馬[2]、皆美 まどか[1]、津久井 脩平[1]、井村 朱里[1]、加藤 悠人[1]、髙橋 直希[1]
*Kenta Kobayashi[1], Keita Takahashi[2], Shun Suzuki[2], Ohashi Kenji[1], Takuma Katori[2], Minami Madoka[1], Shuhei Tsukui[1], Akari Imura[1], Yuto Kato[1], Naoki Takahashi[1]

1. 新潟大学理学部地質科学科、2. 新潟大学大学院自然科学研究科
1. Department of Geology, Faculty of Science, Niigata University, 2. Graduate School of Science and Technology, Niigata University

The Futagawa and the Hinagu fault zones were activated at the time of the 2016 Kumamo earthquake. To understand how fault zones have developed over a long period of time, it is necessary to observe fault zone structures at the macro to microscope scales. We carried out field surveys in the NE-SW trending aftershock area of the earthquake, and analyzed the development of fractures, slip senses, and mineral assemblages at the fault zone.
The main shock (Mw7.0, April 16) occurred along the ENE-WSW trending Futagawa fault. On the other hand, the foreshocks (Mw6.2, April 14; Mw6.0, April 15) occurred along the NE-SW trending Hinagu fault. After the earthquake, many NE-SW~ENE-WSW trending surface ruptures were found along the Hinagu fault. They indicated dextral slip sense. In addition, a bed composed of lower terrace deposits was folded at the north end of the Hinagu fault. The fold hinge was plunging to NE.
Brittle fault rock zones were distributed in the Higo metamorphic rocks (Permian-Triassic). Andesite dikes (Neogene?) were intruded, also deformed along the faults. Most fault planes with NNW~NNE strike, indicated dextral, sinistral, normal and reverse slip senses. XRD analysis showed that the foliated cataclasite derived from pelitic-psammitic gneiss is mainly composed of smectite, kaolinite, chlorite and laumontite. The foliated gouges are abundant in smectite, contain chlorite and laumontite. NE-SW striking remarkable brittle shear zone was also recognized in the Hinagu Formation (Early Cretaceous), indicated dextral slip sense.
Viewed from the kinematics and the alteration process, the macroscale fault zone in the aftershock area has a long history of deformations. Parts of them were selected, and activated at the time of the 2016 Kumamo earthquake.

キーワード：熊本県、日奈久断層、活断層、断層岩
Keywords: Kumamoto Prefecture, Hinagu fault, active fault, fault rocks

混合確率分布を用いた応力逆解析法：別府湾周辺の第四紀小断層群への適用

Stress tensor inversion by using mixture probability distribution: Application to Quaternary meso-scale faults in Beppu area, southwest Japan

*佐藤 活志[1]
*Katsushi Sato[1]

1. 京都大学大学院理学研究科地球惑星科学専攻
1. Division of Earth and Planetary Sciences, Graduate School of Science, Kyoto University

断層の方位による応力逆解析法は地震学や構造地質学の分野で普及している．Hough変換に基づく応力逆解析法（Yamaji et al., 2006，以下Hough法）には，複数の応力を検出でき，不完全な断層データにも適用できる（Sato, 2006）という利点がある．不完全な断層データとは，滑り方向を示す条線が観察できないもの，剪断センス（正断層，逆断層，右横ずれ断層，左横ずれ断層の区別）が不明なものである．Hough法において，地質時代に記録された複数の応力状態を分離して検出する手法は完全には自動化されていない．そこで本研究は，混合確率分布モデルを用いて応力を自動認定する手法を提案する．

応力逆解析に必要な観測データは，断層面の方位と滑り方向（断層スリップデータ）である．断層の滑り方向が剪断応力と平行であるとの仮定に基づけば，１条の断層スリップデータに適合する応力テンソルは，５次元空間（偏差応力空間）の半円弧上の点に相当する（Sato and Yamaji, 2006）．Hough法は，多数の断層に対応する半円弧を重ね合わせて偏差応力空間上に適合度の分布を得た後，適合度のピークの位置を最適応力と見なす．適合度の分布が複数のピークを持つならば，複数の応力テンソルが解として得られる．本研究は適合度の分布に混合確率分布を当てはめることで，ピークの認定を自動化した．前述の半円弧は偏差応力空間で異方的な形状を持つので，異方性を持つ確率分布として５次元Kent分布を採用した．また，ピークの数はベイズ情報量基準に基づいて決定した．

本手法のテストとして，人工断層データを解析した．２つの応力に起因する断層群を混合して解析したところ，２つの適合度のピークが正しく検出された．本手法を，大分県別府湾周辺に分布する更新統碩南層群を切る小断層群に適用した．NNE-SSW引張応力とNNW-SSE引張応力の２つが検出された．上位の更新統大分層群からは，NNE-SSW引張応力のみが検出されたことから，本地域において1 Ma頃に引張方向が変化したことが示唆された．また，NNE-SSW引張応力の信頼範囲をブートストラップ法によって決定すると，主応力軸の68%信頼範囲は30°程度であった．

References
Sato, 2006, Tectonophysics, 421, 319-330.
Sato, K. and Yamaji, A., 2006, Journal of Structural Geology, 2006, 28, 957-971.
Yamaji, A., Otsubo, M. and Sato, K., 2006, Journal of Structural Geology, 28, 980-990.

キーワード：応力逆解析、小断層解析、混合確率分布
Keywords: stress tensor inversion, fault-slip analysis, mixture probability distribution

ニュージーランド南島北部における、2016年Mw 7.8 Kaikoura 地震前後での発震機構解の応力テンソルインバージョンを用いた、広域応力場の変化

Spatiotemporal distribution of regional stress field associated with the 2016 Mw 7.8 Kaikoura earthquake estimated by stress tensor inversion of focal mechanisms in the northern South Island, New Zealand

*佐藤 将[1]、岡田 知己[1]、飯尾 能久[2]、松本 聡[3]、Bannister Stephen[4]、Ristau John[4]、大見 士朗[2,5]、三浦 勉[2]、Pettinga Jarg [6]、Ghisetti Francesca [7]、Sibson Richard[8]
*Tadashi Sato[1], Tomomi Okada[1], Yoshihisa Iio[2], Satoshi Matsumoto[3], Stephen C Bannister[4], John Ristau[4], Shiro Ohmi[2,5], Tsutomu Miura[2], Jarg Pettinga[6], Francesca Ghisetti[7], Richard Sibson[8]

1. 東北大学大学院理学研究科地球物理学専攻地震・噴火予知研究観測センター、2. 京都大学防災研究所、3. 九州大学大学院理学研究院附属地震火山観測研究センター 、4. GNS Science, New Zealand、5. 京都大学防災研究所地震防災研究部門、6. Univerisity of Canterbury, New Zealand、7. Terra Geologica, New Zealand、8. University of Otago, New Zealand
1. Research Center for Prediction of Earthquakes and Volcanic Eruptions, Graduate School of Science, Tohoku University, Japan, 2. Disater Prevention Research Institute, Kyoto University, Japan, 3. Institute of Seismology and Volcanology, Faculty of Sciences, Kyushu University, Japan, 4. GNS Science, New Zealand, 5. Earthquake Hazards Division, Disaster Prevention Research Institute, Kyoto University, Japan, 6. Univerisity of Canterbury, New Zealand, 7. Terra Geologica, New Zealand, 8. University of Otago, New Zealand

The northern South Island and the southernmost North Island of New Zealand occupy the transition region between subduction and transform tectonics along the Pacific-Australia plate boundary, with the Pacific plate subducting beneath the Australian plate obliquely from the northeast. Active seismicity in the northern South Island results from a combination of subduction and transform tectonics. An Mw 7.8 earthquake involving a combination of reverse and mostly dextral strike-slip faulting occurred in the Kaikoura region of northern South Island at 11:02.56 am (UT) on 14 November 2016. In this study, we estimated the spatio-temporal variation of the crustal stress field by stress tensor inversion using focal mechanisms obtained from micro- to moderate-sized earthquakes.
We analyzed the data acquired by a dense seismic array which has been recording over 2 years from 1 April 2013 to April 2015. We determined focal mechanisms using the HASH program (Hardebeck, 2002; 2003) and estimated the spatiotemporal variation of the crustal stress field using SATSI algorithm (Hardebeck and Michael, 2006). During that time period, there were two major seismic clusters; the first, consisting of aftershocks of the 1990 Lake Tennyson earthquake, occurred in the center of the northern South Island, while the second, consisting of aftershocks of the 2013 Cook Strait earthquakes, occurred in the northeast of the northern South Island. For shallow earthquakes, strike-slip type focal mechanisms were dominant. P axes were oriented ~N120E, similar to that found in previous studies (Reyners et al., 1997; Balfour et al., 2005; Sibson et al., 2011; Townend et al., 2012). T axes were oriented NE-SW. For intermediate-deep earthquake, normal, strike-slip, and reverse faulting seems to be mixed. Most of the P axes were oriented NE-SW, which is also consistent with previous studies (Reyners et al., 1997; Townend et al., 2012).
Next, we conducted stress tensor inversion using SATSI algorithm by dividing the earthquakes into three groups; 0-27km depth, 27-40km depth and deeper than 40km. On the 0-27km depth, the σ_1 axis was oriented ~N120E with high accuracy, while for earthquakes deeper than 40km, the σ_1 axis was oriented

~N60E with high accuracy. Therefore the shallow crustal stress orientation differed from the deep orientation which corresponds to the condition within the subducting Pacific plate.
For the 2016 Kaikoura earthquake, we also used the GeoNet CMTs in the period of approximately three months from 14 November 2016 to 31 January 2017 to estimate the regional postseismic stress field using the SATSI algorithm. The GeoNet CMTs show, that most of the events were shallower than 30 km, with event depths increasing northeast from the mainshock hypocenter. There have been almost three major clusters: the first (the C cluster) is almost in the center of the aftershock area, the second (the NE cluster) is northeastern margin of the aftershock area, and the third (the SW cluster) is around the main shock hypocenter. P axes were oriented to E-W in the NE cluster, while oriented to N120E in the C and SW clusters. T axes were oriented to N-S in the NE cluster and oriented to NE-SW in the C and SW clusters.
We conducted stress tensor inversion using the SATSI algorithm for the events in the 0-27km depth The σ_1 axis was oriented E-W in the NE cluster while σ_1 axes were oriented N120E in the C and SW clusters. We compare the stress tensor solutions before and after the Kaikoura earthquake, The orientations of σ_1 axes are similar, but the 95 % confidence range became wider. This reflects a decrease in the magnitude of σ_1 because of the earthquake, with it becoming closer to the magnitude of σ_2.

キーワード：ニュージーランド南島北部、広域応力場、2016年Kaikoura地震、応力テンソルインバージョン
Keywords: Northern south Island of New Zealand, Regional stress field, 2016 Mw 7.8 Kaikoura earthquake, Stress tensor inversion

Fault evolution process related to stress field transition around the Byobuyama fault, central Japan

*香取 拓馬[1]、小林 健太[1]
*Takuma Katori[1], Kenta Kobayashi[1]

1. 新潟大学自然科学研究科
1. Graduate School of Science & Technology, Niigata University

The central Japan is one of the concentrated area of active faults, which consist of the complicated fault geometry system. It has been reported that the origin of such fault zones can be traced back to the formation of cataclasite zone in late Cretaceous to early Paleogene (Oohashi and Kobayashi, 2008; Niwa et al., 2011). But, the fault development history reported in previous researches has lower resolution than the plate motion history, especially in Neogene period. Therefore, we performed structural study focused on the Byobuyama fault, central Japan. The Byobuyama fault is suitable for constraining the age of fault movement because Miocene Mizunami group and Pliocene-Pleistocene Toki Sand and Gravel formation are located around the fault. To reconstruct the history of the fault movement, we performed a detailed investigation along the Byobuyama fault and collected samples for structural and chemical analyses. To understand structural history, paleo-stress fields analysis using the Multiple Inverse Method (Yamaji, 2000) were performed. Chemical analysis with XRD, XGT, SEM-EDS and EPMA-WDS analyses also conducted. Based on these analyses, following results were obtained.

< Stress Fields >

Comparing the data of cross-cutting relationship with the result of paleo-stress analysis, the following transition history details were obtained. Cataclasite formation under WNW-ESE trending compression, vertical trending extension (Stress A) →Fault gouge formation under NNE-SSW trending compression, vertical trending extension (Stress B) →Fault gouge formation under ENE-WSW trending compression, NNW-SSE trending extension (Stress C) →Fault gouge formation under WSW-ESE trending compression, NNE-SSW trending extension (Stress D).

< Deformation and Alteration >

The cataclasites which received stronger deformation were formed at the later stage. Proto cataclasite is composed stilbite vein and ortho cataclasite composed calcite vein. The matrix of the Stress B gouge is composed mainly of illite. In contrast, smectite is abundant in the Stress C and D gouges.

From the above results, it is evident that the Byobuyama fault has experienced tectonic activities of several stages under different stress states, and significant differences in the deformation and alteration mechanisms exist between these stages. It is considered that the timing of the cataclasite formation correspond to Eocene because Stress A condition matches the convergence direction of the Pacific plate at the time (Maruyama et al., 1997). In previous studies within the Tsukiyoshi fault which adjacent to the Byobuyama fault, a reverse fault movement was detected during deposition of the Mizunami group under N-S compression (Khoriya et al., 2003). It is observed that Stress B also corresponds to this event and related to the collision of Izu-Bonin arc (Tsunakawa, 1986). Since Toki sand and gravel formation not experienced Stress C deformation, it is speculated that this event occurred around Pliocene. Finally, it is identified that Stress D correspond to an active fault event because 1) Toki sand and gravel formation encounter the deformation, 2) Stress D state is consistent with the current stress field. These results with high-resolution tectonic history is considered to be an important achievement on constructing structural evolution history of central Japan.

Reference

Oohashi, K. and Kobayashi, K., 2008, Jour. Geol. Soc. Japan, 114, 16-30.
Niwa, M. et al., 2011, Engineering Geology, 119, 31-50.
Yamaji, A., 2000, Jour. Stru. Geol, 22, 441-452.
Maruyama, S. et al., 1997, The Island Arc, 6, 121-142.
Khoriya, Y. et al., 2003, JpGU Meeting 2013 G015-P003.
Tsunakawa, H., 1986, Jour. Geomag. Geoelectr., 38, 537-543.

キーワード：断層発達、応力場、活断層、屏風山断層
Keywords: Fault evolution, Stress field, Active fault, Byobuyama fault

Generation of pseudotachylyte and interseismic plastic deformation in ancient crustal seismogenic fault zones, Yawatahama-Oshima, Ehime, Japan

*小野 藍生[1]、豊島 剛志[2]、小松 正幸
*Aiu Ono[1], Tsuyoshi Toyoshima[2], Masayuki Komatsu

1. 新潟大学大学院自然科学研究科、2. 新潟大学理学部地質科学科
1. Graduate School of Science and Technology, 2. Department of Geology, Faculty of Science, Niigata University

Three pseudotachylyte-producing fault zones develop in Yawatahama-Oshima, Ehime, Japan (Komatsu et al., 1997, 1998). The Yawatahama-Oshima pseudotachylytes and their related fault rocks were formed under greenschist-facies conditions (upper continental crustal conditions) (Komatsu et al., 1997, 1998; Komatsu, 2001). We illustrate generation of the Yawatahama-Oshima pseudotachylyte accompanied by plastic deformation, as a example of ancient seismogenic fault zones in upper crust.
Pressure solution-precipitation structures (pressure solution cleavage accompanied by quartz and feldspar veins) are characteristically abundant in the Yawatahama-Oshima pseudotachylyte-producing fault zones. Modes of occurrence of the Yawatahama-Oshima pseudotachylytes and pressure solution cleavage indicate that seismic slip with pseudotachylyte generation and slow plastic deformation (pressure solution with precipitation) alternated in the same fault zones and along the same fault surfaces. Therefore we can conclude that pressure solution-precipitation is likely one of the principal deformation mechanisms for interseismic plastic deformation and time-dependent strength recovery of the Yawatahama-Oshima pseudotachylyte-producing fault zones. Their strength recovery processes are explained by a solution-precipitation model, which was proposed for the Hidaka pseudotachylytes from the Hidaka metamorphic belt, Hokkaido, by Wada and Toyoshima (2007).

キーワード：シュードタキライト、塑性変形、圧力溶解劈開
Keywords: pseudotachylyte, plastic deformation, pressure solution cleavage

Interseismic plastic deformation in paleo-seismic fault zones under lower crustal conditions at Tonagh Island in the Napier Complex, East Antarctica

*豊島 剛志[1]、重松 紀生[2]、小山内 康人[3]、大和田 正明[4]、角替 敏昭[5]、外田 智千[6]
*Tsuyoshi Toyoshima[1], Norio Shigematsu[2], Yasuhito Osanai[3], Masaaki Owada[4], Toshiaki Tsunogae[5], Tomokazu Hokada[6]

1. 新潟大学理学部地質科学科、2. 産業技術総合研究所活断層・火山研究部門、3. 九州大学大学院比較社会文化研究院環境変動部門、4. 山口大学理工学研究科地球科学分野、5. 筑波大学生命環境系地球進化科学専攻、6. 国立極地研究所
1. Department of Geology, Faculty of Science, Niigata University, 2. Research Institute of Earthquake and Volcano Geology, Geological Survey of Japan, National Institute of Advanced Industrial Science and Technology, 3. Division of Evolution of Earth Environments, Faculty of Social and Cultural Studies, Kyushu University, 4. Graduate School of Science and Engineering for Innovation, Yamaguchi University, 5. Faculty of Life and Environmental Sciences (Earth Evolution Sciences), University of Tsukuba, 6. National Institute of Polar Research

There are severa; granulite-facies paleo-seismic fault zones (PSF) in Tonagh Island, the Napier Complex, East Antarctica (Toyoshima et al., 1999, 2016). In PSF, alternation of thin ultramylonites, cataclasites, pseudotachylytes, and mylonitized pseudotachylytes occur, showing that multiple generations of pseudotachylytes, cataclasites and ultramylonites.
Two types of granulite-facies ultramylonites occur in PSF: type 1 and 2. Microstructures of recrystallized plagioclase and quartz suggest high-temperature or low-strain rate crystal plastic deformation. Microstructures of recrystallized quartz in type 2 ultramylonites suggest high-strain rate crystal plastic deformation. Z-maximum c-axis lattice preferred orientation (LPO) patterns for quartz in type 2 ultramylonites suggest a basal slip system dislocation creep and high-strain rate crystal plastic deformation during interseismic periods. There are two alternative posibilities of deformaition mechanisms of quartz in type 2 ultramylonites as follows: (1) Mylonitized quartz layers originated from quartz veins parallel to mylonite foliation. (2) Water weakening occurred during mylonitization of quartz. Microstructures and LPO patterns of recrystallized plagioclase indicate switch in deformation mechanism from dislocation creep to grain-boundary sliding in type 2 ultramylonites, and also suggest that continuous low strain rate or low differential stress plastic deformation and seismic events alternated. This is imaged acceleration of strain rate or stress relaxation before or after seismic events, respectively. The switch in deformation mechanism from dislocation creep to grain-boundary sliding, associated with the grain-size reduction, attests of the mechanical softening during deformation, which contributed to the localization of the strain within the mylonite, as suggested by Raimbourg et al. (2008).

キーワード：シュードタキライト、高歪速度結晶組成変形、粒界すべり
Keywords: pseudotachylyte, high-strain rate crystal plastic deformation, grain boundary sliding

The role of fracturing in the formation of lower crustal shear zones

*奥平 敬元[1]
*Takamoto Okudaira[1]

1. 大阪市立大学大学院理学研究科地球学教室
1. Department of Geosciences, Graduate School of Science, Osaka City University

Plagioclase-rich rocks are major constituents of the lower crust, and then understanding the rheological properties and deformation processes of plagioclase-rich rocks is key to evaluating the strength and mechanical behavior of the lower crust. Investigating grain size reduction and possible subsequent grain-size-sensitive (GSS) deformation in plagioclase-rich rocks is particularly important because a transition to GSS creep would result in significant rheological weakening. Dynamic recrystallization is a common grain-size reduction mechanism in plagioclase aggregates deformed by grain-size-insensitive (GSI) dislocation creep under conditions of the amphibolite to granulite facies. Empirical relationships between stress and recrystallized grain size have been proposed for plagioclase aggregates. If such stress and grain size relations transect the boundary between GSI and GSS creep fields, grain size reduction by dynamic recrystallization can lead to a transition from GSI dislocation creep to GSS creep. However, in the GSS creep field the applicability of the empirical piezometer is problematic owing to a potential lack of driving force for recrystallization. Dynamic recrystallization may represent a balance between grain size reduction and crystal growth processes set up in the boundary region between the GSI and GSS creep fields, and then recrystallized grain size and stress balance near the GSI–GSS field boundary. Thus, major weakening in localized natural deformation zones is unlikely to be caused by dynamic recrystallization. Fracturing and/or comminution are dominant grain-size reduction mechanisms at low temperatures because the critical resolved shear stress may not be reached in plagioclase, and recovery and recrystallization are limited. However, even under high-temperature conditions where plagioclase undergoes plastic deformation, fracturing and nucleation of new grains as small fragments has been identified in naturally and experimentally deformed rocks. Zones of very fine grains that result from fracturing and/or comminution would deform by GSS creep and then would develop as ductile shear zones in the lower crust. In this study, we summarized the *P–T* conditions of dynamic recrystallization and fracturing in the lower crustal plagioclase-rich rocks, and will discuss the formation and development of shear zones in the lower crust.

キーワード：レオロジー、下部地殻、剪断帯、破砕作用、動的再結晶、斜長石
Keywords: Rheology, Lower crust, Shear zone, Fracturing, Dynamic recrystallization, Plagioclase

Importance of fault rheology around brittle-plastic transition in long-term behavior of major faults

*野田 博之[1]
*Hiroyuki Noda[1]

1. 京都大学防災研究所
1. Kyoto University, Disaster Prevention Research Institute

Fault behavior such as long-term slip rate, magnitude and recurrence interval of earthquakes, and reaction against stress perturbation depends on the loading condition and mechanical properties of the fault. In considering the latter factor, existence of a ductile shear zone, which underlies a seismogenic part of a major fault, may be of great importance; the brittle-plastic transitional regime has maximum shear resistance in a classical Christmas-tree strength profile, and the slip there directly load the shallower seismogenic part of the fault. In order investigate the long-term, time-averaged fault behavior, numerical simulations of earthquake sequences on a major fault with a ductile shear zone have been conducted in the present study in a simplified geometry.

An elastic crustal plate with a through-going strike-slip fault is assumed, and the fault motion is driven by applying constant far-field shear stress tau_pl. A rate- and state-dependent friction-to-flow fault constitutive law [Shimamoto and Noda, 2014] is used in the present study. In this law, shear resistance is approximately given by a rate- and state-dependent friction law in a shallow brittle part of the fault, and by power-law creep of quartzite (exponent: 4) in a deep, fully plastic part. The rate-dependency of the shear resistance takes the maximum value in a transitional regime between them. Note that the peak in the rate-dependency does not necessarily correspond with peak shear resistance. If we assume excess pore pressure at depth which limits the effective normal stress at a certain value, then a Christmas-tree strength profile does not exist, but a remarkable peak in the rate-dependency still appears in the transitional regime.

In the simulations, the fault hosts repeating earthquakes in the brittle part, and slips by a long-term speed V_pl on average which depends on tau_pl. The relation between tau_pl and V_pl is very well explained by a power law with the exponent about 20. This is similar to what is followed by unstable steady-state solutions with uniform slip rates V_ss. It should be noted that V_pl is larger than V_ss for the same tau_pl approximately by a factor of 2 as long as studied. This is because the brittle part of the fault typically support smaller shear stress than the steady-state level, and thus the ductile shear zone support larger shear stress associated with larger slip rate than the steady state. Since the relation between tau_pl and V_ss is given by spatial average of the rate-dependency, the transitional regime having the prominent peak in the rate-dependency most significantly contributes to the amount of shear stress perturbation required to change the long-term slip rate of the fault. It should be emphasized that the brittle-plastic transitional regime is important not only because of the maximum strength potentially existing there, but also because of the maximum rate-dependency.

キーワード：脆性塑性遷移、地震サイクル、断層の長期的滑り速度
Keywords: Brittle-plastic transition, Earthquake sequence, Long-term fault motion

Fracture contact state inferred from longitudinal wave velocity: Theoretical and experimental approach

*Eranga Gayanath Jayawickrama[1], Hayata Tamai[2], Jun Muto[1], Hiroyuki Nagahama[1]

1. Department of Earth Science, Tohoku University, 2. East Japan Railway Company

Seismic tomography has provided many important details of the earth’ s interior in the past few decades and variation in wave velocity has been a key factor in understanding the seismograms. Therefore, by velocity inversions the understanding of low velocity zones within the earth’ s crust has been improved and in general these low velocity zones are identified as zones with fluids or geologically weak zones. In reflection seismology, low velocities can be identified as weak zones, basically as fractures. Even though these inversions have the ability to show the fractured zones, they have not been able to show the degree of opening of the fractures. Therefore, to understand the fracture contact state, it is important to achieve a relationship between the contact state and the velocity, so that by the variation in velocity the contact state can be inferred.

As to the current knowledge, the elastic wave velocity is highly affected by the fractures, and this indicates that the contact state has a strong influence over the variation in velocity. The wave velocity increases as the contact state changes its relative displacement with increasing pressure. This change in displacement was explained by Nagumo (1963) for different types of single contacts. In this study, we have extended this pressure-displacement relationship of single contacts to a velocity-pressure relationship, and discuss the multiple contact state variation inferred from the change in velocity with increasing pressure.

From one dimensional wave equation, a power law relationship of longitudinal wave velocity and pressure is introduced with a pressure exponent representing the contact state of fractures. For single cone, ball and flat contacts, the pressure exponent λ takes values of 1/2, 1/3 and 0, respectively. By extending this to multiple contacts the pressure exponent μ representing multiple contacts have been deduced as 2/3, 3/5 and 1/2 for multiple cone, ball and flat contacts, respectively. Using previously published experimental data and an empirically derived equation (Kobayashi and Furuzumi, 1972) which is similar to the theoretically derived relationship in the current study, the applicability of the theory is tested. From the results, we show that the contact state changes form conical contacts, to ball contacts and finally to flat contacts with increasing pressure.

The study has also shown that the lithology, microstructures and presence of water are factors that control the contact state with increasing pressure. Granite and gabbro show pressure exponents $\mu < 1/2$ indicating complete closure of fractures while serpentinite is yet to close completely at the same pressure. Also, rocks with equally low porosity but different lithologies show different contact states at equal pressures. These indicate that lithology is a major factor controlling the contact state. Further a marked difference in contact states can be observed depending on the direction of measurement with respect to the foliation and depending on the water existence. The velocity change with increasing pressure also can be explained in terms of contact state of fractures using the current contact state theory since the prominent velocity change is mimicked by an equally prominent contact state change at the same pressure.

As shown from our study, this method is applicable to assess the contact state of fractures in an area of interest. By obtaining velocity data from reflection seismology and seismic tomography, and using the wave velocity-contact state relationship introduced here, the degree of fracture opening can be estimated. Therefore, we believe this method can be used in wide range of applications from shallow depth exploration geophysics to understanding the anomalies in lower crust.

Keywords: Contact state, Fractures, Wave velocity

Microstructures and quartz c-axis fabrics in granitic protomylonite from the Median Tectonic Line fault zone, Mie Prefecture, south-west Japan

*Dong Van Bui[1], Toru Takeshita, Jun-ichi Ando, Takafumi Yamamoto

1. Department of Natural History Sciences, Graduate School of Science, Hokkaido University

During major orogenic events, the conditions and mechanisms of deformation play an important role in their development. Deformation conditions and histories can be obtained from various microstructures in constituting mineral phases of deformed rocks. Among them, quartz c-axis fabrics in quartz-rich tectonites are the very useful indicators. In this study, we will report microstructures and quartz c-axis fabrics from granitic protomylonite to mylonite, which occur along the Median Tectonic Line (MTL), Mie Prefecture, south-west Japan, and infer deformation conditions and histories during the development of the MTL.
The MTL is a major strike slip fault system with the largest structural break in southwestern Japan that has been defined as the boundary fault between Sambagawa metamorphic rocks and Ryoke granitic and metamorphic rocks. Protomylonite in the MTL was derived from granitoids in the Ryoke belt in the latest Cretaceous called the Kashio phase, before the MTL was formed as the boundary fault during the exhumation of the Sambagawa metamorphic rocks at 63-58Ma (Kubota and Takeshita, 2008).
Protomylonite from the MTL, which suffered cataclasis to a certain degree, consists of quartz ribbons and feldspar porphyroclasts in a matrix consisting of finely-crushed quartz and feldspar porphyroclasts, chloritized mafic minerals, muscovite altered from plagioclase, and calcite veins. The feldspar porphyroclasts show many extension fractures with $\sigma 1$ being perpendicular to the foliation. Some of the feldspar porphyroclasts are decorated by recrystallized feldspar grains along grain boundaries. The quartz ribbons are large and strongly flattened relic grains showing undulatory extinction, deformation lamellae, and fluid inclusion arrays, surrounded by very-fine recrystallized quartz grains indicating buldging recrystallization (Stipp et al., 2002). Type III and type IV deformation twin of calcite (Burkhard, 1990) dominate in the calcite veins.
The c-axis orientation distribution of large quartz grains was measured by a scanning electron microscope (SEM; JEOL JSM6390A) equipped with an electron backscatter diffraction (EBSD) detector, which mostly shows a Y maximum with type II crossed girdles indicating dominant operation of prism {10-10} slip system and a type I crossed girdle pattern with r-maxima for a small number of samples indicating the dominant operation of rhomb {1011} slip (Tullis, 1977; Lister and Hobbs, 1980; Schmid and Casey, 1986; Law, 1990; Heilbronner and Tullis, 2002; Takeshita et al. 1999; Okudaira et al. 1995).
The crystallographic orientation map of recrystallized quartz grain, which was measured by the EBSD mapping with step size of 1 micrometer, illustrated many subgrain boundaries and small recrystallized grains surrounded by larger recrystallized grains, suggesting a strong overprinting recrystallization at higher differential stresses. Two groups of recrystallized quartz grain occur in the protomylonite samples: the larger and the smaller recrystallized quartz grains with the size of approximately 70 micrometer and 10 micrometer, respectively. Further, several sizes of dynamically recrystallized fine-grained quartz are observed at the peaks of approximately 20 micrometer and 45 micrometer.
The Y-max quartz c-axis fabric associated with the coarse-grained recrystallized quartz (70 micrometer) could indicatite the deformation temperatures in protomylonite samples around intermediate temperatures (400-500 °C), whereas the fined-grained recrystallized quartz (10 micrometer) could have formed at temperatures of 300-400 °C based on the paleostress estimation from recrystallized quartz grain size (e.g. Stipp and Tullis, 2003) and constitutive equations of flow in quartz aggregates (e.g.

Gleason and Tullis, 1995). Thus, overprinting deformation could have occurred in these protomylonites along the MTL, represented by the reduction of recrystallized quartz grain size from c. 70 micrometer to c. 10 micrometer with several peak sizes of dynamically recrystallized fine-grained quartz. This overprinting deformation could have occurred heterogeneously in both spatial and temporal development during the exhumation of protomylonite along the MTL.

Keywords: Microstructures, Quartz c-axis fabrics , Protomylonite, The MTL

Frictional properties of the Median Tectonic Line fault zone

*高橋 美紀[1]、稲生 千咲[2]、亀田 純[3]、重松 紀生[1]
*Miki Takahashi[1], Chisaki Inaoi[2], Jun Kameda[3], Norio Shigematsu[1]

1. 国立研究開発法人　産業技術総合研究所活断層・火山研究部門、2. 北海道大学大学院理学院自然史科学専攻、3. 北海道大学大学院理学研究院自然史科学専攻
1. Institute of Earthquake and Volcano Geology, Geological Survey of Japan, AIST, 2. Department of Natural History Sciences, Graduate School of Science, Hokkaido University, 3. Earth and Planetary System Science Department of Natural History Sciences, Graduate School of Science, Hokkaido University

We investigated frictional properties of fault gouges of the Median Tectonic Line (MTL) at an outcrop (Awano-Tabiki outcrop) exposed in the eastern Kii Peninsula, Japan, using a laboratory experiment technique to evaluate a strength-history of the MTL fault. Shigematsu et al., (2017) described that the MTL fault zone at Awano-Tabiki outcrop is suffered four stages of faulting under different depthes in brittle regime. The newest deformation at the Awano-Tabiki outcrop (stage 4) is characterized by a localized zone with a normal faulting sense of slip within ~ 1 cm in thickness (gouges-B and F). Those gouges are rich in smectite, indicating that the depth to activate the MTL fault at this stage would be relatively shallow at which the temperature is lower that 140 deg.C. On the other hand, the oldest deformation (stage 1) is widely distributed in such as gouges D, I-L with a dextral sense of slip. They are rich in muscovite and illite, indicatiing that corresponding temperature could be higher than 200 deg.C. Therefore to investigate frictional property of each fault gouge at each deformation condition based on mineral compositions, could be a key to reveal a history of a crustal fault strength such as the MTL fault. An experimental machine we used was a gas-medium, high-pressure, high-temperature triaxial apparatus set at GSJ, AIST, Japan. We set initially temperature conditions, *T*, to 100 deg.C for gouge-B and gouge-F and to 250 deg.C for gouge-D, respectively. Then, confining pressures, *Pc*, corresponding to assumed depth were determined by assumed geothermal gradient (20~60 deg.C/km). We thought conditions of pore pressure, *Pp*, and sliding velocity, *V*, would change in the earthquake cycle. We, therefore, varied the values of *Pp* (hydrostatic ~ Pc) and *V* (0.011 mm/sec ~ 115 mm/sec for stepwise change). After 75 mm mesh sieving, 0.6 g of smaller-grain-sized powder sample of the gouge was sandwiched between porous alumina pre-cut blocks, which provided c.a. 0.5 mm thick gouge layer. The powder samples of gouge-B and gouge-F contained 24 wt.% and 34 wt.% of smectite, respectively. On the othre hand, the powder sample of gouge-D was rich in muscovite (26 wt.%) and illite (21 wt.%), but did not contain the smectite. We obtained interesting results on both the shear strength and the velocity dependence of friction for those smectite rich gouges. Average values of friction coefficient, showing a dependence of the smectite content, are 0.30 for gouge-B and 0.18 for gouge-F. However, the friction coefficient for both gouges became decreasing significantly towards ~0.05 at *Pc-Pp* < c.a. 14 MPa, while the frictional coeffcient on gouge-D showed a constant value of 0.42 with no effective pressure dependence. Common properties of the gouges were that the velocity dependence of friction became positive at high *V*, low *Pp* and high smectite content but became negative at the low *V*, high *Pp* and low smectite content.
We will, thus,add cases for other samples of gouge zones formed between oldest stage generating gouge-D and newesrt stage generating gouge-B and –F to complete a figure for the strength-history of the MTL fault.

キーワード：断層ガウジ、中央構造線断層、速度依存性、摩擦係数
Keywords: fault gouge, the Median Tectonic Line fault, velocity dependence of the friction, friction coefficient

静岡県東部，富士川層群浜石岳層中に産出する変形礫岩のレオロジーと成因 -変形礫岩に記録された衝突帯のテクトニクス-
Study of rheology and origin of deformed conglomerates, Pliocene Hamaishidake Formation Fujikawa Group, Eastern part of Shizuoka prefecture, Central Japan -Tectonics of the collision zone recorded deformed conglomerate-

*鈴木 俊[1]、小林 健太[1]
*Shun Suzuki[1], Kenta Kobayashi[1]

1. 新潟大学大学院自然科学研究科
1. Graduate School of Science & Technology, Niigata University

南部フォッサマグナは，フィリピン海・ユーラシア・北アメリカプレートの会合部にあたり，日本でも屈指の変動帯である．また，フィリピン海プレート上の伊豆-小笠原弧の本州弧への多重衝突・付加の場としても注目を集めている．本研究地域に広く分布する富士川層群浜石岳層（上部中新統～鮮新統）は，衝突現象に伴って形成されたトラフを充填した堆積物で，礫岩や火山砕屑物を主体とした地層である．これらの分布東限には活断層である富士川河口断層帯入山断層・芝川断層（総延長26km以上）がほぼNSトレンドで延び，さらに東側の庵原層群（更新統）とを境する．これらの断層群の南方延長はそのまま駿河トラフに接続するとされる（杉山・下川，1982など）．よって，直近のトラフ充填堆積物中には，プレート境界部における複雑な構造運動の痕跡が記録されていることが期待される．さらに近年，浜石岳層中の礫岩層において外形が流動を伴いつつ脆性変形を受けた面状カタクレーサイトの露頭が報告された（丸山，2008）．これまで浜石岳層からの面状カタクレーサイトの産出は知られていないことから，連続性や成因に関しても不明なままである．そこで本研究では，衝突帯におけるテクトニクスの解明を目的として，先述した面状カタクレーサイト露頭の基本的な記載およびそれらを軸とした各種解析を行った．

面状カタクレーサイト（富士川剪断帯）は，静岡県富士宮市南西部の富士川にかかる新内房橋付近の河床に，東西30m・南北300ｍにわたって広く露出する．変形は一様ではなく何条かの変形集中帯が観察される．地層の走向と剪断帯のトレンドはほぼ平行である．それらの基本トレンドはN45°～60°Wであるが，一部EWトレンドも認められる．礫の変形様式は，非変形の礫から剪断変形が卓越する礫・外形が流動するような礫（Cataclastic flow）まで多種多様であり，これらが共存して産する．礫のファブリックから求められる剪断センスは左横ずれを示すものが多い．剪断帯の連続性については今回の調査では認められず．周辺地質ではNS系の褶曲構造や断層ガウジを伴うような脆性変形が卓越的であることが明らかになった．また，各所にて断層面の構造測定を行い，多重逆解法（山路，2000）を用いて古応力の復元を試みた．その結果，剪断帯においてはNNE-SSW σ1の横ずれ応力場，周辺の断層ガウジからはEW σ1の逆断層応力場，入山断層直近の破砕帯からはWNW-ESE σ1の左横ずれ応力場が卓越的に検出された．

以上のような記載・解析の結果，剪断帯は周辺地質のNS系の基本構造とは明らかに斜交するNW-SE方向の基本構造を持って，局所的な分布で産出することが明らかになった．また，断層岩の形成レジューム深度の観点から考えると，剪断帯とその周辺地質の変形様式には明らかなギャップが存在する．仮に剪断帯が断層ガウジ形成レジューム深度よりもより深部で形成されたものと考えるならば，剪断帯のNW-SE方向の構造は周辺のNS系の褶曲構造を切断しているため，褶曲形成後に局所的な地質体の上昇イベントがあったことが考えられる．応力解析結果より，本研究地域にはまず剪断帯を形成するようなNNE-SSW圧縮の横ずれ応力場が働いていた．地質体の上昇と共にそれらはNS系の褶曲構造形成に寄与したEW圧縮に転化し， NS系の断層群は逆断層として活動した．その後，WNW-ESE圧縮の横ずれ応力場で入山断層は左横ずれ運動を開始し，トレース付近

において幅広い破砕帯を形成したと考えられる．本発表では，このような記載・解析結果からプレート境界部における地質構造発達史について議論する．

キーワード：南部フォッサマグナ、多重衝突帯、富士川河口断層帯、変形礫、断層岩
Keywords: South Fossa Magna, multiple collision zone, Fujikawa estuary fault zone, deformed conglomerate, fault rocks

かんらん石細粒多結晶体の焼結
sintering polycrystalline olivine from pulverized olivine crystals

*坪川 祐美子[1]、石川 正弘[1]
*Yumiko Tsubokawa[1], Masahiro Ishikawa[1]

1. 横浜国立大学大学院 環境情報
1. Faculty of Environment and Information Sciences, Yohokohama National University

The rheological properties of Earth’ s interior have been determined by laboratory experiments of polycrystalline samples of rock-forming minerals. In these deformation experiments, fine-grained specimens are often required for deformation in diffusion creep regime at laboratory strain rates (e.g. Karato, 2010). In this study, we successfully fabricated olivine nano-sized powder from naturally occurring olivine single crystal (peridot:$Mg_{1.76\sim1.84}Fe_{0.16\sim0.24}SiO_4$). In order to investigate a method for preparing fine-grained and highly dense nanocrystalline olivine, the sintering behavior of olivine powder was studied. Olivine powder were pressed into cylindrical shape and sintered under argon flow at temperatures ranging from 1130-1350 ℃ for 2-6 hours. After the sintering, sample surfaces were polished and thermally etched to expose grain boundaries. Grain size and porosity were determined from the microstructure of scanning electron microscope. Olivine grains in sintered samples are polygonal and isotropic shape, and show a homogeneous structure. The average grain size increased with increasing sintering time and sintering temperature, and a significant grain growth was found for the sample sintered at 1350 ℃. At temperatures of 1300 ℃, we could obtain dense polycrystalline olivine with an average grain size of < 2 μm.

キーワード：焼結、かんらん石、多結晶体
Keywords: sintering, olivine, polycrystsalline

Viscosity and graphitic carbon weakening of diopside

*石川 正弘[1]、坪川 祐美子[1]
*Masahiro Ishikawa[1], Yumiko Tsubokawa[1]

1. 横浜国立大学大学院環境情報研究院
1. Graduate School of Environment and Information Sciences Yokohama National University

Dynamic behaviours of Earth‘s plates are strongly dependent on the viscosity of Earth‘s upper mantle. Although a trace amount of hydrogen can markedly weaken the upper mantle, the influence of carbon on viscosity of the upper mantle is unknown. Here we report the deformation experiment of diopside, one of the main constituents of the upper mantle. In order to investigate influence of graphite on creep properties of diopside, we prepared graphite-bearing nano-polycrystalline diopside (average grain size ϕ=0.4μm). Deformation experiments have been carried out on graphite-bearing nano-polycrystalline diopside in argon gas atmosphere in a uniaxial deformation apparatus. A homogeneous shortening was observed when the graphite-bearing nano-polycrystalline diopside specimen was compressed at 1080 ℃ and 1060 ℃ under subsolidus conditions. The stress exponent n=1.08 at 1080 ℃ suggests that the deformation mechanism of the graphite-bearing nano-polycrystalline diopside is dominated by diffusion creep rather than dislocation creep. Viscosity of the graphite-bearing nano-polycrystalline diopside (1.00-1.25 x 10^{11} Pa s at 1080 ℃) is much lower than that of graphite-free diopside aggregates. Our results demonstrate that diopside is weakened by a small amount of graphite.

キーワード：ディオプサイド、グラファイト、炭素、粘性、焼結、ナノ
Keywords: diopside, graphite, carbon, viscosity, sinter, nano

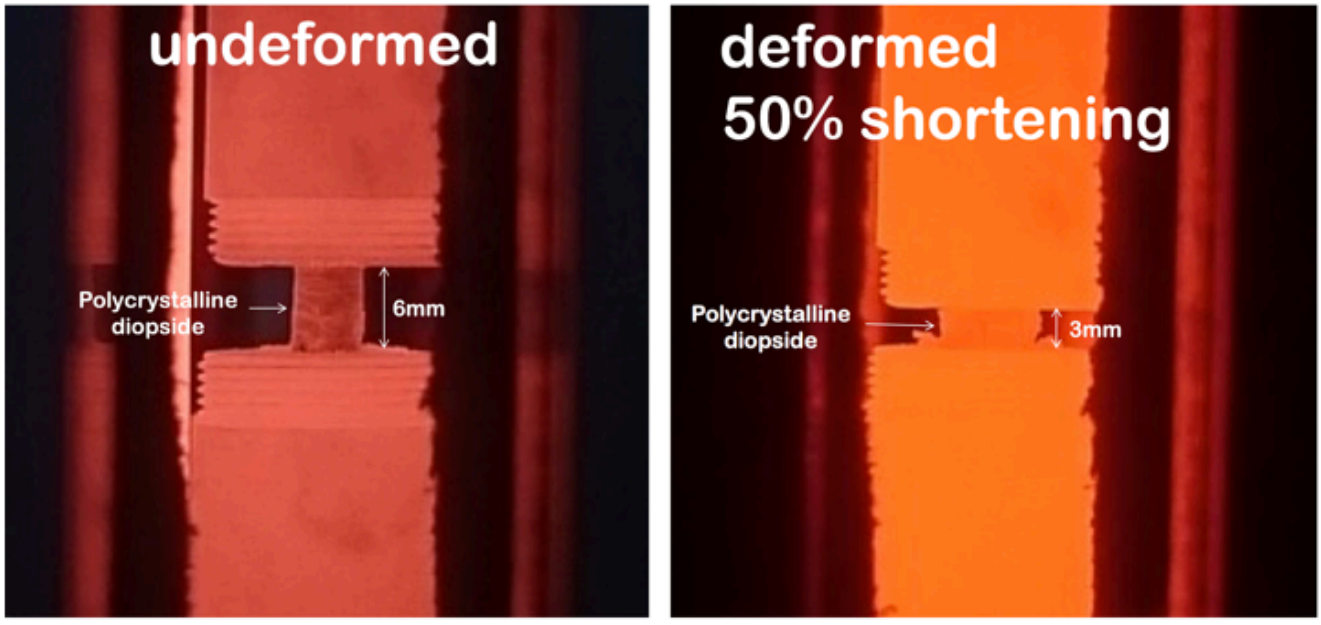

Fabrication of albite aggregate by hot pressing

*重松 紀生[1]、周 游[2]、日向 秀樹[2]、吉澤 友一[2]
*Norio Shigematsu[1], You Zhou[2], Hideki Hyuga[2], Yuichi Yoshizawa[2]

1. 国立研究開発法人産業技術総合研究所活断層・火山研究部門、2. 国立研究開発法人産業技術総合研究所構造材料研究部門
1. Research Institute of Earthquake and Volcano Geology, Geological Survey of Japan, National Institute of Advanced Industrial Science and Technology, 2. Structural Materials Research Institute, National Institute of Advanced Industrial Science and Technology

Feldspar is one of the main constituent minerals of the Earth’ s crust. The mechanical behavior of plastic deformation of feldspar has previously well studied especially for anorthite ($CaAl_2Si_2O_8$), because this controls the strength of the lower crust. On the other hand, several studies of natural fault rocks and experimental results suggest that plagioclase with composition close to albite ($NaAlSi_3O_8$) shows complicated transient behaviors of plastic deformation which possibly control the shear localization and the nucleation of fractures in the crust. In this study, we examined a method to fabricate aggregate of albite to examine such properties experimentally in future.
Albite powders for glaze were pulverized using an automatic pulverizer (HERZOG HSM-250A at AIST Tsukuba Central 7) and fine-grained fractions were separated by decantation. The fine-grained powders were hot pressed by a multi-purpose high temperature furnace (Fuji Dempa High Multi 10000 at AIST Chubu). To determine the condition for fabrication, several fractions of particle size from a few hundred nm to 1 micrometer were prepared. Experiments were carried out at temperatures of 1000-1150°C and pressures of 40-100 MPa. For comparison, we have also carried out a sintering at the atmospheric pressure after formation.
Fabrication of dense albite aggregate is difficult due to the lower diffusion coefficient and melting temperature. The run products were partially melted in the experiments at the temperatures higher than 1100°C. The run products were porous and were not completely sintered in the experiments using powders with particle size of 1 micrometer. Even in the experiments using powders using a few hundred nm, it takes about a hundred hours to fabricate dense aggregate under the pressure of 40 MPa and the temperature of 1100°C, although the materials were partially melted. We succeeded to fabricate dense aggregate without melt phase in the experiment using powders with particle size of a few hundred nm under the pressure of 100 MPa and the temperature of 1080 °C for 36 hours.
Above mentioned results indicate that using fine particle size less than a few hundred nm, temperature of around 1080°C and the pressure above 100 MPa are essential for dense fabrication. There is a possibility that microstructures of aggregate controls the complicated transient behaviors expected for albite. We further explore the method to fabricate the aggregates with various microstructures.

キーワード：曹長石、ホットプレス、材料合成、焼結
Keywords: albite feldspar, hot pressing, fabrication, sintering

Fluid flow governed by fault zone architecture, the Alpine Fault, New Zealand

*重松 紀生[1]、マシオット セシール[2]、タウンエンド ジョン[2]、ドーン マイリーン[3]、マクナマラ デイビッド[4]、トイ バージニア[5]、スザランド ルーパート[2]、DFDP-2 サイエンスチーム
*Norio Shigematsu[1], Cecile Massiot[2], John Townend[2], Mai-Linh Doan[3], David D. McNamara[4], Virginia Toy[5], Rupert Sutherland[2], DFDP-2 Science Team

1. 独立行政法人産業技術総合研究所活断層・火山研究部門、2. ビクトリア大学ウェリントン、3. グルノーブル大学、4. アイルランド国立大学ゴールウェイ校、5. オタゴ大学
1. Research Institute of Earthquake and Volcano Geology, Geological Survey of Japan, National Institute of Advanced Industrial Science and Technology, 2. Victoria University of Wellington, 3. University of Grenoble, 4. National University of Ireland, Galway , 5. University of Otago

Fracture pattern within a fault zone controls and records a wide range of crustal processes. However, these fractures usually reflect the complicated history of reactivation, and it is difficult to reveal how the fractures were formed. The Alpine Fault provides a unique opportunity to overcome this problem because the hangingwall uplift rate is very rapid, implying that all fractures in the hangingwall have not experienced the fault reactivation (e.g., Little., et al., 2005).
The DFDP-2B borehole was drilled in late 2014 in the hangingwall of the Alpine Fault and a series of wireline logging was acquired (Sutherland et al., 2015). The orientations of planar structures in the hangingwall of the Alpine Fault were revealed by the analysis of acoustic borehole televiewer (BHTV) logs (Massiot et al., 2017). In this study, fracture pattern near the Alpine Fault was examined based on the orientations of fractures revealed by the BHTV logs. Unfortunately, drillcore samples were not recovered due to technical problems during the drilling.
Fractures were formed or slipped in response to ambient stress. In this study, a technique of stress tensor inversion was applied to the orientations of fractures to characterise the fracture pattern. Reduced stress tensors were inferred with assuming the Wallace-Bott hypothesis based on fault slip data. Different fracture patterns should yield different solutions of reduced stress tensor. However, fracture orientation based on BHTV are not usually complete fault slip data without slip directions, although truncated features in BHTV logs occasionally constrain slip directions. For this reason, we compute stress parameters using the Hough transform method (Yamaji et.al., 2006). We assume that fractures with similar geometries to the Alpine Fault accommodated similar top-to-the-west shear, and that other fractures have reverse fault components.
2244 planar structures were detected in BHTV logs, and 1680 of them can be interpreted as fractures. Stress tensors were determined for groups of fractures within 20 m depth intervals. The analyses in depth intervals shallower than 730 m (measurement depth) yield orientations (trend/plunge) for the maximum and minimum compressive stress axes S1 and S3 of about 120/20 and 020/30 (±30˚), respectively and a stress ratio of (S2−S3)/(S1−S3)=0.3−0.4, while those in depth intervals deeper than 730 m yield S1 and S3 axes of about 310/10 and 050/45 (±30˚), respectively and a stress ratio of (S2−S3)/(S1−S3)= 0.7. Solution of stress tensor, i.e., fracture pattern, changes at ~730 m depth. The thermal profile measured by distributed temperature sensing (DTS) using a fibre-optic cable indicates that a thermal gradient also changes at ~730 m depth.
The dataset of fractures deeper than 730 m characteristically includes shallowly SE dipping structures. Orientations of these structures correspond to the R_1 shear of the Alpine Fault, which are often developed in fault damage zones. In general, damage zones of fault zones have high permeability compare to the surrounding rocks and fault core (e.g., Cain et al., 1996; Lockner et al., 2009). It can be considered that

rock and fluid advections play key role to account for the thermal profile of DFDP-2B (Sutherland et al., submitted). Therefore, there is a possibility that the deflection in the thermal profile at ~730 m depth corresponds to the boundary of the damage zone of the Alpine Fault. The results of fracture pattern and the thermal profile suggest fluid flow governed by the fault zone architecture of the Alpine Fault.

キーワード：亀裂パターン、ボアホールテレビューア、アルパイン断層、 DFDP-2B 、応力テンソル逆解析
Keywords: fracture pattern, acoustic borehole televiewer, The Alpine Fault, DFDP-2B , stress tensor inversion

Influence of water fugacity on flow properties of fine-grained anorthite aggregates under the lower crustal conditions

*木戸 正紀[1]、武藤 潤[1]、小泉 早苗[2]、長濱 裕幸[1]
*Masanori Kido[1], Jun Muto[1], Sanae Koizumi[2], Hiroyuki Nagahama[1]

1. 東北大学大学院理学研究科地学専攻、2. 東京大学地震研究所
1. Department of Earth Science,Tohoku University, 2. Earthquake Research Institute, The University of Tokyo

Fluids in deep part of the crust have an important role in deformation and seismicity of the crust. In particular, water has great influence on rheological properties of rocks and minerals. Significant reductions of flow strength caused by water have been discovered for dominant mineral constituents of the crust and mantle (e.g., Griggs and Blacic, 1965). Flow strength is affected by water fugacity which rises sharply under the pressure corresponding to the lower crust. However, experimental data of crustal materials under the lower crustal conditions are insufficient.
In this study, we performed high temperature and high pressure deformation experiments to reveal rheological properties of feldspar under hydrous conditions. Axial compression tests on synthetic polycrystalline anorthite aggregates with 0.5 wt% of water were performed in a Griggs-type solid medium deformation apparatus at temperature of 900 ˚C and various confining pressures of 0.8-1.4 GPa. Times were changed to investigate the reduction of strength by diffusion of water into samples. Water contents incorporated in the samples were measured by a Fourier-transformed infrared spectroscopy (FTIR) method.
Strengths of wet anorthite tended to decrease with increasing time or strain magnitude. It was suggested that anorthite samples were still not saturated with water in time range of this study. Strengths of wet anorthite also decreased with increasing confining pressures. Differential stresses were significantly lower than predicted values by previous flow laws for wet anorthite obtained by low pressure experiments (<0.5 GPa). This implies that the effect of fugacity of water on strength in higher pressure might be larger than those predicted by lower pressure experiments (e.g., Rybacki et al., 2006). Our experiments show that the strength of hydrous rocks in the lower crust becomes lower than that predicted by previous studies.

キーワード：レオロジー、水のフュガシティ、細粒灰長石多結晶体
Keywords: rheology, water fugacity, fine-grained anorthite aggregates

高圧・高温における塩水の見かけの誘電率：予報
Apparent dielectric constants of brines at high P-T conditions: A preliminary report

*星野 健一[1]、盛田 唯花
*Kenichi Hoshino[1], Yuika Morita

1. 広島大学大学院理学研究科地球惑星システム学専攻
1. Department of Earth and Planetary Systems Science, Hiroshima University

地殻流体は一般に，水−塩（−ガス成分）の混合流体であろう。このような混合溶媒中と水溶媒中の溶質jの化学ポテンシャルの差（$D\mu^{\circ}_{j}$）は，

$D\mu^{\circ}_{j} = \omega_{j} (1/\varepsilon_{m} - 1/\varepsilon_{w})$,

と示される。ここで，ω_{j}は溶質jのボルン係数で，ε_{m}とε_{w}はそれぞれ混合溶媒と水の誘電率である。従って，溶媒の誘電率は，溶媒の化学的性質を決定する鍵となる。言い換えると，混合溶媒の誘電率がわかれば，例えばSUPCRT92などから得られる水溶媒中の溶質の熱力学的状態量から，混合溶媒中のそれらを求めることができる。

これまでの高圧・高温における石英の溶解度測定実験では，H_2O-NaCl系溶媒中の溶解度が水に比べて高い場合（塩溶）と低い場合（塩析）があることが示されてきた。この効果は，上式で示されるSiの主要な溶存種である$SiO_{2(aq)}$のH_2O-NaCl系溶媒と水溶媒中の化学ポテンシャルの差で説明できるであろう。即ち，塩溶が生じる場合はH_2O-NaCl系溶媒の誘電率が水より大きく，塩析の場合はその逆であるはずである。圧が50 - 200 MPa，温度が200 - 550℃の範囲で，NaClモル濃度が0.5 - 1.6程度のH_2O-NaCl系溶媒中の上記溶解度のほとんどは，水溶媒中のそれより高い，即ち，塩溶が生じている。

これらの実験データと，低温（＜50℃）のH_2O-NaCl系溶媒で提唱されている誘電率を用いて，圧が50 - 200 MPa，温度が25 - 550℃の範囲の1モルNaCl溶媒の見かけの誘電率（ε_{b}）と水の誘電率（ε_{w}）の比を求めた。

$\varepsilon_{b} / \varepsilon_{w} = a / (2 \pi b)^{0.5} \exp(- (T - c)^2 / (2 b)) + d$,

ここで，piは円周率，Tは絶対温度で，a，b，cおよびdはそれぞれ定数で，300，13000，573および0.8であり，上記の範囲では圧に依存しない。この式が示すように，塩溶効果は300℃付近で最も大きくなり，100℃と500℃付近で効果は消滅する。

これを用いて，100 MP 定圧で，500℃から200℃まで温度が降下する場合の，石英に飽和した水溶媒と1モルNaCl溶媒からの温度25℃降下当たりの石英の沈殿量を求めた。その結果，水溶媒の場合では400℃（425℃から400℃に降下）で最も沈殿量が大きいが，その量は475℃の場合より30%ほど大きいに過ぎない。これに対して1モルNaCl溶媒の場合では，350℃付近で最も大きく，475℃の場合の約9倍にも上る。

予察的な解析ではあるが，この結果は，地殻流体が塩水の場合には，裂かの充填や熱水変質などの塩水−岩石相互作用が，350℃付近で著しく進展することを示している。

キーワード：誘電率、塩水、水ー岩石相互作用
Keywords: dielectric constant, brine, water-rock interaction

紀伊半島のMT法による3次元地殻流体分布
Three-dimensional geofluid distribution of Kii Peninsula, SW Japan

*木下 雄介[1]、小川 康雄[1]、齋藤 全史郎[1]、野口 里奈[1]、藤田 清士[2]、山口 覚[3]、梅田 浩司[4]、浅森 浩一[5]、市來 雅啓[6]
*Yusuke Kinoshita[1], Yasuo Ogawa[1], Zenshiro Saito[1], Rina Noguchi[1], Kiyoshi Fuji-ta[2], Satoru Yamaguchi[3], Umeda Koji[4], Koichi Asamori[5], Masahiro Ichiki[6]

1. 東京工業大学、2. 大阪大学、3. 大阪市立大学、4. 弘前大学、5. 日本原子力研究開発機構、6. 東北大学
1. Tokyo Institute of Technology, 2. Osaka University, 3. Osaka City University, 4. Hirosaki University, 5. Japan Atomic Energy Agency, 6. Touhoku University

Although Kii peninsula is located in the forearc side of southwest Japan, it has high temperature hot springs and fluids from mantle are inferred from the isotopic ratio of helium. Non-volcanic tremors underneath the Kii Peninsula suggest rising fluids from slab.
Previously, in the southern part of the Kii Peninsula, wide band magnetotelluric measurements were carried out (Fujita et al. ,1997; Umeda et al. ,2004). These studies could image the existence of the conductivity anomaly in the shallow crust and in the deep crust. Long period observation using network MT data showed low resistivity on wedge mantle(Yamaguchi et al., 2009). These studies, however, used two dimensional inversions and three-dimensionality is not fully taken into consideration.
As part of the “Crustal Dynamics” project, we have measured 20 more stations so that the whole wide-band MT stations constitute grids to make three-dimensional modeling of the area.

In total we have wide-band magnetotelluric sites. Preliminary 3d inverse modeling showed the following features.
(1) The high resistivity in the eastern Kii Peninsula at depths of 5-40km. This may imply consolidated magma body of Kumano Acidic rocks underlain by resistive Philippine Sea Plate which subducts with a low dip angle.
(2) The northwestern part of Kii Peninsula has the shallow low resistivity in the upper crust.
(3) The northwestern part of the survey area has a deeper conductor in the lower crust to upper mantle.This reflects the Phillipine Sea subduction with higher dip angle.

3D magnetotelluric imaging of fluid distribution in a seismogenic region, Miyagi, NE Japan

齋藤 全史郎[2]、*小川 康雄[1]、市來 雅啓[3]、佐藤 秀幸[4]、木下 雄介[2]、鈴木 惇史[2]、Amatyakul Puwis[1]
Zenshiro Saito[2], *Yasuo Ogawa[1], Masahiro Ichiki[3], Hideyuki Satoh[4], Yusuke Kinoshita[2], Atsushi Suzuki[2], Puwis Amatyakul[1]

1. 東京工業大学理学院火山流体研究センター、2. 東京工業大学地球惑星科学専攻、3. 東北大学大学院理学研究科、4. 産業技術総合研究所
1. Volcanic Fluid Research Center, School of Science, Tokyo Institute of Technology, 2. Earth and Planetary Sciences, Tokyo Institute of Technology, 3. Graduate School of Science, Tohoku University, 4. National Institute of Advanced Industrial Science and Technology

Northern Miyagi is located in one of the strain concentration zones in NE Japan. This area is well known to have high seismicity and experienced two large earthquakes, the 1962 Northern Miyagi Earthquake (M6.5) and the 2003 Northern Miyagi Earthquake (M6.2). The 2003 earthquake was well studied and its focal mechanism and aftershock distribution support that the earthquake was a high angle reversed fault, which is a reactivation of an originally normal fault, created in the Miocene during the Japan opening. The surface extension of the fault is recognized as a flexure. Geologically, the area is mostly simply covered with thick sediment and is surrounded by granitic rocks of Kitakami Mountains to the east and to the north. The objective of this study is to image the geofluid in three dimensions and relate them to earthquake activities in the region. The previous studies have done by 2D modeling. We used MT data at 67 sites in total: 39 sites are new, 24 sites of them are arranged in an approximately 2 km grid and other 15sites are along E-W profile above the focal area of the 2003 Northern Miyagi earthquake, whereas two older dataset were along profiles, one NEE-SWW profile with 16 sites (Mitsuhata et al., 2001), and one NNE-SSW profile with 12 sites (Nagao, 1997). We inverted the data using WS3dMTINV (Siripunvaraporn and Egbert, 2009). The model showed that two shallow (less than 10km depth) and three deep (deeper than 10km) conductors exist: One of shallow conductors represent sedimentary layers. The thickest part is located around Izu-Numa in the northwestern part of the study area. Another is westward dipping conductor as fractured zone of the fault. The hypocenters of the aftershocks of 1962 earthquake distribute at the deeper extension of this dipping conductive layer. deep conductors are located at more 10km depth near the focal area of the 1900, 1962 and 2003 Northern Miyagi earthquake, respectively. The seismic activity is seen at shallower side of the border between itself and high resistivity anomaly. The deep conductors may imply an anomalous body containing saline fluids originating from slab fluids. And, we noticed that seismic activity is high around the deep conductors covered by high-resistivity, especially, along the fault. This may suggest the episodic migration of fluid from the fluid reservoir to the upper brittle crust triggers high seismicity.

キーワード：地殻流体、比抵抗、マグネトテルリック法、宮城県北部地震
Keywords: fluid, electrical resistivity, magnetotellurics, Northern Miyagi Earthquake

Simultaneous measurements of elastic wave velocity and electrical conductivity in fluid-bearing granitic rocks under confining pressures

*貝羽 洋平[2]、今野 綾[2]、出合 絵璃菜[2]、寺西 伽羅[2]、渡辺 了[1]
*Yohei Kaiwa[2], Aya Konno[2], Erina Deai[2], Kyara Teranishi[2], Tohru Watanabe[1]

1. 富山大学大学院理工学研究部、2. 富山大学理学部地球科学教室
1. Gradudate School of Science and Engineering, University of Toyama, 2. Department of Earth Sciences, University of Toyama

Geophysical mapping of fluids is critical for understanding crustal processes. Seismic velocity and electrical resistivity structures have been revealed to study the fluid distribution. However, the fluid distribution has been still poorly constrained. Observed velocity and resistivity should be combined to make a quantitative inference on fluid distribution. The combined interpretation requires a thorough understanding of velocity and resistivity in fluid-saturated rocks. We have studied elastic wave velocities and electrical conductivity in brine-saturated granitic rocks under confining pressures.
Aji granite (Aji, Kagawa Pref., Japan) and Oshima granite (Oshima, Ehime Pref., Japan) were selected as rock samples for textural uniformity. Cylindrical samples (D=26 mm, L=30 mm) were evacuated and filled with 0.1 M KCl aqueous solution. Velocity and electrical conductivity were simultaneously measured by using a 200 MPa hydrostatic pressure vessel. The pore-fluid was electrically insulated from the metal work by using teflon devices. The confining pressure was progressively increased up to 150 MPa, while the pore-fluid pressure was kept at 0.1 MPa. It took 3 days or longer for the electrical conductivity to become stationary after increasing the confining pressure.
Velocity and conductivity showed reproducibly contrasting changes with increasing confining pressure. Elastic wave velocities increased by less than 10% as the confining pressure increased from 0.1 MPa to 50 MPa, while electrical conductivity decreased by an order of magnitude. The changes must be caused by the closure of cracks under pressure. The large change at low pressures shows that there lots of cracks with small aspect ratios ($<10^{-3}$). Both velocity and conductivity showed no remarkable changes at higher pressures. The large conductivity change at low pressures must be related to the percolation of cracks.

キーワード：地震波速度、電気伝導度、流体
Keywords: seismic velocity, electrical conductivity, fluid

Change in electrical conductivity in a brine-saturated granite under uni-axial compression

澤城 凌[2]、*渡辺 了[1]、渡邉 真也[2]
Ryo Sawaki[2], *Tohru Watanabe[1], Watanabe Shinya[2]

1. 富山大学大学院理工学研究部、2. 富山大学理学部地球科学教室
1. Gradudate School of Science and Engineering, University of Toyama, 2. Department of Earth Sciences, University of Toyama

Geophysical observations have shown that fluids exist pervasively within the crust. Fluids fill intergrain cracks (open grain boundaries) and intra-grain cracks at the upper and middle crust conditions. Since the opening of cracks strongly depends on the stress state, electrical conductivity should be anisotropic under a stress state. We have conducted uni-axial compression tests on brine-saturated granitic rocks and studied the change in electrical conductivity in the directions parallel and perpendicular to the compression.
The loading system is composed of a hand press (Maximum load: 20 kN), a load cell and stainless steel end-pieces. A fine grained (100-500 mm) biotite granite (Aji, Kagawa Pref., Japan) was selected as a rock sample for its small grain size and textural uniformity. A cube sample with the edge length of 25 mm was filled with 0.1 M KCl aqueous solution and loaded up to 20 MPa. Electrical impedance was continuously monitored during a compression test with two-electrode method (Ag-AgCl electrodes).
Electrical conductivity decreased with increasing axial stress in the directions parallel and perpendicular to the compression. Electrical conductivity decreased in both directions with increasing axial stress, and the conductivity change was almost reversible. No significant difference in the magnitude of conductivity change was observed between two directions. The decrease in conductivity must be caused by the closure of cracks, which were perpendicular or subperpendicular to the compression. The fluid path for the electrical conduction in the axial direction must be composed of cracks parallel and perpendicular to the axial stress. Electrical conductivity does not become anisotropic, while elastic wave velocity does.

キーワード：差応力、電気伝導度、異方性
Keywords: differential stress, electrical conductivity, anisotropy

Pressure dependence of electrical conductivity in brine-saturated Berea sandstone and its pore structure

*南部 美菜子[1]、渡辺 了[2]
*Minako Nambu[1], Tohru Watanabe[2]

1. 富山大学大学院理工学教育部、2. 富山大学大学院理工学研究部
1. Graduate School of Science and Engineering for Education, University of Toyama, 2. Graduate School of Science and Engineering, University of Toyama

Electrical conductivity in brine-sturated Berea sandstone (porosity~20%) was measured under confining pressures of up to 100 MPa. The pore-fluid pressure was kept at the atmospheric pressure (0.1 MPa). Electrical conductivity decreased by 22% as the confining pressure was increased to 40 MPa. Volumetric strain of a dry rock sample was separately measured under confining pressures. The volume change was 0.7% as the confining pressure was increased to 50 MPa. The change in porosity should be only 1%. The observed relatively large decrease in conductivity shows that the connectivity of pores in the porous Berea sandstone was significantly reduced by a small decrease in porosity. In order to understand the nature of the conduction path, the pore structure in Berea sandstone was observed with X-ray CT conducted at Tokyo Metropolitan Industrial Technology Research Institute. 3D images of pores were constructed by processing X-ray CT images to examine the connectivity of pores.

キーワード：電気伝導度、砂岩、空隙構造
Keywords: electrical conductivity, sandstone, pore structure

